

547807  
P86

**NASA Technical Memorandum** 101617  
**AVSCOM Technical Memorandum** 89-B-004

**INTEGRATED MULTIDISCIPLINARY  
OPTIMIZATION OF ROTORCRAFT:  
A PLAN FOR DEVELOPMENT**

**Edited by**

**Howard M. Adelman and Wayne R. Mantay**

(NASA-TM-101617) INTEGRATED  
MULTIDISCIPLINARY OPTIMIZATION OF  
ROTORCRAFT: A PLAN FOR DEVELOPMENT  
83 p

May 1989

(NASA)  
CSCL 01C

63/05

N90-12580  
--THRU--  
N90-12588  
Unclas  
0220012

**NASA**

National Aeronautics and  
Space Administration

**Langley Research Center**  
Hampton, Virginia 23665-5225



**US ARMY  
AVIATION  
SYSTEMS COMMAND**  
AVIATION R&T ACTIVITY

# CONTENTS

	PAGE
Foreword .....	iii
Preface .....	iv
Introduction .....	1
General Approach and Scope .....	351
Rotor Blade Aerodynamic Design .....	10-952
Rotor Blade Dynamic Design .....	1353
Rotor Blade Structural Design .....	1754
Acoustic Design Considerations .....	2255
Airframe Design Considerations .....	2756
Validation of the Procedures .....	31-30
Schedule and Milestones .....	35-57
Concluding Remarks .....	36
Appendix - Results Obtained to Date .....	38
Aerodynamic Performance Optimization .....	38
Dynamic Optimization .....	40-53
Optimum Locations of Vibration Tuning Masses .....	42
Rotor Structural Optimization .....	43
References .....	46

## FOREWORD

Interdisciplinary analysis and optimization methods offer significant benefits to aircraft and spacecraft design and performance. Development and validation of these methods is a high payoff and a challenging research opportunity. Recent trends in industry, academia, and government research laboratories show an increasing interest in using discipline integration methods in engineering design. From our contacts, we are aware of the growing interest in the development and application of mathmatically-based, design optimization procedures. This interest is especially strong in the design of rotorcraft. Rotorcraft is one of the areas where an integrated, multidisciplinary design approach offers excellent potential for productivity and performance gains.

The development plan outlined in this document represents a focussed attempt to develop a logic path for the difficult case of helicopter rotor systems, where aerodynamics, structures, dynamics, and acoustics all interact. We expect the outcome of this activity to be an understanding and formulation of the logic elements required for the fully optimized design.

We endorse the integrated rotorcraft analysis and design activity outlined in this research plan. We place strong emphasis on the validation of the analytical and optimization methods that we expect to be developed. Any software developed during this work is designed only to exercise the methodology and is not intended as deliverable product of the activity. We offer this plan to the rotorcraft research community for their study and critique. Suggestions for improving the plan are welcome, particularly in the areas of concept validation. We hope this plan will stimulate dialog and increase the interest in the important area of discipline integration methods.



Charles P. Blankenship  
Director for Structures  
NASA Langley Research Center



Wolf Elber  
Director, US Army  
Aerostructures Directorate  
Langley Research Center

## PREFACE

This paper represents the combined efforts of members of a team of researchers and managers at the NASA Langley Research Center and US Army Aerostructures Directorate involved in analysis and optimization of rotorcraft. The writing of the various sections of the paper was divided among the persons listed below along with their NASA-Langley, Army, and local corporate organizational affiliations:

Howard M. Adelman	Interdisciplinary Research Office
Aditi Chattopadhyay	Analytical Services & Materials, Inc.
Raymond G. Kvaternik	Structural Dynamics Division
Wayne R. Mantay	Aerostructures Directorate
Ruth M. Martin	Acoustics Division
T. Sreekanta Murthy	Planning Research Corporation
Mark W. Nixon	Structural Dynamics Division
Kevin W. Noonan	Aerostructures Directorate
Jocelyn I. Pritchard	Interdisciplinary Research Office
Joanne L. Walsh	Interdisciplinary Research Office

## INTRODUCTION

An emerging trend in the analytical design of aircraft is the integration of all appropriate disciplines in the design process (refs. 1 and 2). This means not only including limitations on the design from the various disciplines, but also defining and accounting for interactions so that the disciplines influence design decisions simultaneously rather than sequentially. Because the terms "integrated" and "discipline integration" are frequently used imprecisely, we offer the following definition of an integrated disciplinary design process. Such a process is integrated if:

- (1) Information output from any discipline is expeditiously available to all other disciplines as required.
- (2) The effect of a design variable change proposed by one discipline on all other disciplines and the system as a whole is made known promptly.

Adhering to the above definitions is central to the plan to be described in this paper. The integrated approach has the potential to produce a better product as well as a better, more systematic design process. In rotorcraft design (the rotor in particular), the appropriate disciplines include aerodynamics, dynamics, structures, and acoustics. The purpose of this paper is to describe a plan for developing the logic elements for helicopter rotor design optimization which includes the above disciplines in an integrated manner.

Rotorcraft design is an ideal application for integrated multidisciplinary optimization. There are strong interactions among the four disciplines cited previously; indeed, certain design parameters influence all four disciplines. For example, rotor blade tip speed influences dynamics through the inertial and air loadings, structures by the centrifugal loadings, acoustics by local Mach number and air loadings, and aerodynamics through dynamic pressure and Mach number. All of these considerations are accounted for in current design practice. However, the process is usually

sequential, not simultaneous, and often involves correcting a design late in the design schedule.

Applications of rigorous and systematic analytical design procedures to rotorcraft have been increasing, especially in the past five years. Procedures have accounted for dynamics (refs. 3-8), aerodynamics (ref. 9), and structures (ref. 10). Generally, these applications have only considered single-discipline requirements, although in reference 5, dynamic and structural requirements were considered together, and in reference 6, dynamics and aeroelastic stability were combined.

In early 1985, several occurrences led to an excellent opportunity at the NASA Langley Research Center to address the multidisciplinary design problem for rotorcraft. The Interdisciplinary Research Office was established and charged with the development of integrated multidisciplinary optimization methods. Nearly concurrently, the Army Aerostructures Directorate at Langley established the goal of improving rotorcraft design methodology by "discipline integration." Close cooperation between the NASA and Army organizations led to initial plans for a comprehensive, integrated analytical design capability. A group of NASA/Army researchers recently formed a committee and began detailed planning for this activity. The committee, designated IRASC (Integrated Rotorcraft Analysis Steering Committee), has now completed the bulk of the planning and has formulated the approach described in this paper.

The development of an integrated multidisciplinary design methodology for rotorcraft is a three-phased approach. In phase 1, the disciplines of blade dynamics, blade aerodynamics, and blade structures will be closely coupled, while acoustics and airframe dynamics will be decoupled from the first three but will be accounted for by effective constraints on the other disciplines. In phase 2, acoustics will be integrated with the first three disciplines. Finally, in phase 3, airframe dynamics will be fully integrated with the other four disciplines. In all three phases, systematically validated methods are the principal products.

This paper is primarily concerned with the phase 1 activity; namely, the rigorous mathematical optimization of a helicopter rotor system to minimize a combination of horsepower required at various flight conditions and hub shear transmitted from the rotor to the fuselage. The design will satisfy a set of design requirements (constraints) including those on blade frequencies, autorotational inertia, aerodynamic performance, and blade structural constraints. Additionally, the design is required to satisfy constraints imposed by response of the fuselage and also those constraints related to acoustics requirements.

GENERAL APPROACH AND SCOPE

Howard M. Adelman and Wayne R. Mantay

N90-12581  
S, -05  
220013  
547801  
P8  
88

The general approach for the activity is illustrated in figure 1. In phase 1 the blade aerodynamic analysis, blade dynamics, and blade structural analysis are coupled and driven by the optimizer. The optimization of the blade aerodynamic geometry as well as the internal structure (spar, leading and trailing edge, ballast, etc.) takes place inside the box in figure 1. The influences of the airframe dynamics and acoustics are accounted for in terms of design requirements (constraints) on the blade design. These requirements are described in the next section of the paper. For a check on the efficacy of representing the acoustics requirements indirectly, the "final" design will be input to an acoustics analysis. The acoustics analysis calculates the acoustic constraints and derivatives of these constraints with respect to the design variables. This information will be used to determine how well the design was able to satisfy the actual acoustics design requirements.

The phase 2 procedure, wherein acoustics is fully integrated with the blade aerodynamics, blade dynamics, and blade structural analysis, is also illustrated in figure 1. The design produced in phase 2 (when converged) will satisfy acoustics goals. Airframe dynamics in phase 2, as in phase 1, is accounted for by effective constraints on the blade dynamics, aerodynamics, and structural behavior. Finally,

in phase 3 airframe dynamics is integrated and the result is a fully integrated optimization strategy.

This section of the paper consists of details of the integrated rotorcraft optimization problem. Included are descriptions of the following: the objective function (the quantity to be minimized for obtaining an optimum design); the design variables (dimensions and other parameters of the design); constraints (a set of behavioral or characteristic limitations required to assure acceptable and safe performance); and definitions of the interactions among the disciplines.

#### Objective Function

The objective function will consist of a combination of the main rotor horsepower at five flight conditions plus a measure of vibratory shear transmitted from the rotor to the hub. Although several multiple objective function techniques are available (ref. 11) one leading candidate is a linear combination whereby

$$F = k_1HP_1 + k_2HP_2 + k_3HP_3 + k_4HP_4 + k_5HP_5 + k_6S \quad (1)$$

where  $F$  is the objective function

$k_1$  through  $k_6$  are weighting factors

$HP_1$  through  $HP_5$  are required horsepower at various flight conditions

$S$  is the vertical hub shear

A candidate set of flight conditions would be:

<u>Flight condition</u>	<u>Description</u>	<u>Velocity (kts)</u>	<u>Load factor</u>
1	Hover	0	1.0
2	Cruise	140	1.0
3	High speed	200	1.0
4	Maneuver	120	3.5
5	Climb	1000 fpm (VROC)	-

## Blade Model and Design Variables

Figure 2 is a depiction of the rotor blade model to be used in the phase 1 optimization activity. Also shown in figure 2 are the design variables which are defined in table 1. The blade model may be tapered in both chord and depth. The depth is linearly tapered from root to tip. The chord is constant from the root to a spanwise location (referred to as the point of taper initiation) and may be linearly tapered thereafter to the tip. Design variables which characterize the overall shape of the blade include the blade radius, point of taper initiation, taper ratios for chord and depth, the root chord, the blade depth at the root, the flap hinge offset, and the blade maximum twist. Tuning masses located along the blade span are characterized by the mass values and locations. Design variables which characterize the spar box beam cross section include the wall thicknesses at each spanwise segment and the ply thickness at  $0^\circ$  and  $\pm 45^\circ$ . Additional design variables include the number of rotor blades, the rotor angular speed, and the distribution of airfoils.

## Constraints

As previously described, the phase 1 activity is based on integrating the blade aerodynamic, dynamic, and structural analyses within the optimization procedure. The acoustics and airframe dynamics analyses are decoupled from the first three disciplines and their influences are expressed in terms of constraints. Accordingly, the total set of constraints is made up of two subsets. The first subset consists of constraints which are evaluated directly from the first three disciplinary analyses and are a direct measure of the degree of acceptability of the aerodynamic, dynamic, and structural behavior. The second subset represents indirect measures of the satisfaction of constraints on the acoustics behavior and the requirement of avoiding excessive vibratory excitation of the airframe by the rotor.

The constraints are summarized in table 2. The first two constraints are for aerodynamic performance and require that for all flight conditions, main rotor

horsepower not exceed available horsepower and that airfoil section stall not occur at any azimuthal location. The next nine constraints address blade dynamics. The first requires that the blade natural frequencies be bounded to avoid approaching any multiples of rotor speed. The next five impose upper limits on the blade vertical and inplane loads, transmitted hub shear, hub pitching, and rolling moments. The next three dynamic constraints are an upper limit on blade response amplitude, a lower limit on blade autorotational inertia, and finally, the aeroelastic stability requirement. The structural constraints consist of upper limits on box beam stresses, blade static deflection, and blade twist deformation. The acoustic constraints are expressed as an upper bound on the tip Mach number and an upper bound on the blade thickness to limit thickness noise; and an upper bound on the gradient of the lift distribution to limit blade vortex interaction (BVI) and loading noise. The effective airframe constraints are expressed first as a separation of the fundamental blade inplane natural frequency in the fixed system from the fundamental pitching and rolling frequency of the fuselage. Second is a bounding of the blade passage frequency to avoid the proximity to any fuselage frequency. The final constraint is an upper limit on the blade mass which will avoid any designs which satisfy the constraints at the expense of large mass increases.

### Interdisciplinary Coupling

Phase 1 of the effort will utilize several design variables which have historically been significant drivers of disciplinary phenomena. In addition, other variables are being included to provide other unexplored design opportunities. Table 3 shows an attempt to quantify the interactions among the disciplines through the design variables. For example, rotor tip speed has driven past rotor designs based solely on acoustics, performance, or dynamics. This variable also influences blade structural integrity and fixed system response to transmitted loads. This provides the strong interdisciplinary coupling for tip speed shown in table 3. There

are variables, such as blade twist, which can strongly influence some disciplines, such as aerodynamics, while not perturbing others (e.g., structures) and other variables such as a hinge offset which, heretofore, have not greatly influenced conventional rotor design.

A significant part of the current effort will explore not only the obvious strong design variable couplings, but will also address those variables which may provide design synergism for multidisciplinary design goals. This may provide a design key for missions which have not been accomplished with today's rotorcraft.

### Organization of System

The overall organization of the system to optimize a blade design for aerodynamics, dynamics, and structural requirements is shown schematically in figure 3. In order to perform the aerodynamic, dynamic, and structural analyses indicated in the blocks in figure 3, it is first necessary to transform or "pre-process" the design variables into quantities needed in the various analyses. For example, the dynamic and structural analyses both need stiffnesses  $EI$  and  $GJ$ , and laminate properties. The aerodynamic analysis needs lift and drag coefficients for the airfoils used. The above information is obtained by the design variable pre-processors which act as translators of the global design variables into local variables needed in the analyses. The output of each analysis block, in general, serves two purposes. First, response-type output may be transmitted to another analysis block (e.g., airloads from aerodynamics to dynamics); second, information entering into the objective function or constraints is supplied to the objective function and constraints block (e.g., stress constraints from the structural analysis). A key part of the procedure is the sensitivity analysis. This block corresponds to the calculation of derivatives of the constraints and objective function with respect to the design variables. The derivatives quantify the effects of each design variable on the design and,

thereby, identify the most important design changes to make enroute to the optimum design.

The sensitivity data are passed to the optimizer along with the current values of the design variables, constraints, and objective function. The optimizer uses the information to generate a new set of design variables, and the entire procedure is repeated until a converged design is obtained. For our purposes, a design is converged when all constraints are satisfied and the objective function has reached a value which has not changed for a specified number of cycles.

#### Optimization Algorithm

The basic optimization algorithm to be used in this work is a combination of the general-purpose optimization program CONMIN (ref. 12) and piecewise linear approximate analyses for computing the objective function and constraints. Since the optimization process requires many evaluations of the objective function and constraints before an optimum design is obtained, the process can be very expensive if complete analyses are made for each function evaluation. However, as Miura (ref. 3) points out, the optimization process primarily uses analysis results to move in the direction of the optimum design; therefore, a complete analysis needs to be made only occasionally during the design process and always at the end to check the final design. Thus, various approximation techniques can be used during the optimization to reduce costs. In the present work, the objective function and constraints will be approximated using piecewise linear analyses that consist of linear Taylor series expansions.

CONMIN.- CONMIN is a general-purpose optimization program that performs constrained minimization using a usable-feasible directions search algorithm. In the search for new design variable values, CONMIN requires derivatives of the objective function and constraints. The user has the option of either letting CONMIN determine the derivatives by finite differences or supplying such derivatives to CONMIN. The

second option will be used in this work. Analytical derivatives will be used whenever possible - for example for vibration frequencies, mode shapes, and modal shear. Eventual incorporation of the Global Sensitivity Equation (GSE) approach is planned. As described in reference 13, the GSE approach is potentially very effective for integrated problems such as a helicopter rotor. Finite difference schemes will be used for derivative calculations where analytical approaches are unavailable.

Piecewise linear approximation.- In the approximate analysis method, derivatives of the objective function and constraint functions with respect to the design variables are used for linear extrapolation of these functions. The assumption of linearity is valid over suitably small changes in the design variable values and will not introduce a large error into the analysis provided the changes remain small.

Specifically, the objective function  $F_o$ , the constraints  $g_o$ , and their respective derivatives are calculated for the design variables  $V_{o,k}$  using an accurate analysis. For example the aerodynamic performance constraints are supplied by CAMRAD (ref. 14). The first-order Taylor series approximations for the new objective function and the constraint values are as follows:

$$F = F_o + \sum_{k=1}^{NDV} \frac{\partial F}{\partial V_k} (V_k - V_{o,k}) \quad (2)$$

and

$$g = g_o + \sum_{k=1}^{NDV} \frac{\partial g}{\partial V_k} (V_k - V_{o,k}) \quad (3)$$

where NDV is the number of design variables,  $F$  is the extrapolated value of the objective function,  $g$  is the extrapolated value of the constraint, and  $V_k$  is the updated design variable value determined by CONMIN.

Errors introduced by the piecewise linear approach are controlled by imposing "move limits" on each design variable. Move limits are specified as fractional

changes in each design variable value. Additional information and examples of the piecewise linear analysis is given in reference 15.

ROTOR BLADE AERODYNAMIC DESIGN

Joanne L. Walsh and Kevin W. Noonan

N90-12582  
5205 547810  
20014 P4

This section of the paper deals with the aerodynamic performance aspects of rotor blade design. Design considerations, aerodynamic constraints and design variables are described.

Design Considerations

An important aspect of aerodynamic design of a helicopter rotor blade is the selection of the airfoils which could be applied over various regions of the blade radius. The choice of airfoils is controlled by the need to avoid exceeding the section drag divergence Mach number on the advancing side of the rotor disc, avoid exceeding the maximum section lift coefficients on the retreating side of the rotor disc, and avoid high oscillatory pitching moments on either side of the rotor disc. Since airfoils with high maximum lift coefficients are advantageous in high speed forward flight and pull-up maneuvers, high lift sections are generally used from the rotor blade root out to the radial station where the advancing side drag divergence Mach number precludes the use of the section. From that station outward, other airfoil sections which have higher drag rise Mach numbers are used.

Once the airfoils and an initial airfoil distribution are selected, the induced and profile power components become functions of twist, taper ratio, point of taper initiation, and blade root chord (ref. 16). For the hover condition, the majority of the power is induced power and the remainder is profile power. Rotor blade designs which minimize both induced and profile power are desirable. The induced power is a function of blade radius, chord, and section lift coefficient. The profile power is a function of blade radius, chord, and section drag coefficient. The induced and profile power can be reduced (provided the aerodynamics of all retreating blade

air-foils are within linear theory) by increasing taper ratio and/or blade twist - both of which tend to increase inboard loading and decrease tip loading. Configurations which increase tip loading may be efficient at very high speeds under certain design constraints (such as a maximum allowable blade radius) but these kinds of configurations will not be considered in phase 1 of this activity.

Satisfactory aerodynamic performance is defined by three requirements. First, the required horsepower for all flight conditions (see eq. 1) must not exceed the available horsepower. Second, airfoil section stall along the rotor blade must be avoided for any forward flight operating condition, i.e. the airfoil sections distributed along the rotor blade must operate at section drag coefficients less than a specified value (neglecting the large drag coefficients in the reverse flow region). Third, the helicopter must be trimmed in forward flight.

#### Rotor Blade Aerodynamic Constraints

The first design requirement translates into five constraints of the type shown below. BY CONMIN sign convention, a constraint  $g_i$  is satisfied if it is negative or zero and violated if it is positive.

$$g_1 = \text{HP}_r / \text{HP}_a - 1 \quad \text{hover} \quad (4)$$

$$g_2 = \text{HP}_r / \text{HP}_a - 1 \quad \text{cruise} \quad (5)$$

$$g_3 = \text{HP}_r / \text{HP}_a - 1 \quad \text{high speed} \quad (6)$$

$$g_4 = \text{HP}_r / \text{HP}_a - 1 \quad \text{maneuver} \quad (7)$$

$$g_5 = \text{HP}_r / \text{HP}_a - 1 \quad \text{climb} \quad (8)$$

where  $\text{HP}_r$  and  $\text{HP}_a$  are the total horsepower required and the total horsepower available for the main rotor, respectively.

The second design requirement - that airfoil section stall not occur - translates into constraints on the airfoil section drag coefficient ( $c_d$ ) at various

azimuthal angles for the various flight conditions. At a given azimuthal angle  $\psi$  the constraint is formulated as follows:

$$g = \left( c_{d_{1,\psi}} / c_{d_{\max}} \right) - 1 \quad (9)$$

where  $c_{d_{\max}}$  is the maximum allowable drag coefficient and  $c_{d_{1,\psi}}$  is the largest drag coefficient along the blade radius outside the reverse flow region at a given azimuthal angle (see figure 4).

The third design requirement, that the helicopter must be trimmed for each forward flight condition, is somewhat difficult to translate into a continuous mathematical programming constraint. This constraint is implemented by determining from the aerodynamic analysis whether or not, at a specified velocity, the helicopter can trim at the specified gross weight.

#### Analyses

Two analysis computer programs are used to predict rotor performance. The hover analysis denoted HOVT (which uses a strip theory momentum analysis, described in ref. 16 and ref. 17) will be used to compute hover and climb horsepower. The CAMRAD program (ref. 14) will be used to define the trim condition, the horsepower required in forward flight, and the airfoil section drag coefficients for the forward flight and maneuver conditions. Both analyses use tables of experimental two-dimensional airfoil data. The choice of CAMRAD was based on several considerations. First, CAMRAD is being coupled with computational fluid dynamics (CFD) analyses which will result in better modeling of transonic and other effects (ref. 18); replacing CAMRAD with a CFD-coupled version of CAMRAD should cause a minimum amount of changes to the total optimization program compared to the substitution of an entirely different global performance analysis. Second, CAMRAD was selected for the loads and stability computations, so using it for the forward flight aerodynamic analysis streamlines the overall analysis flow. The hover performance trends predicted by HOVT have been

verified by model tests of both advanced and baseline designs for the UH-1, AH-64, and UH-60 helicopters (refs. 19-22). A more sophisticated hover analysis which includes wake effects may be used in the future if the trends predicted by such an analysis are verified for a wide range of configurations, i.e., different taper ratios, taper initiation points, twist distributions, etc.

547811 P5  
N90-12583

#### ROTOR BLADE DYNAMIC DESIGN

Jocelyn I. Pritchard, Howard M. Adelman, Wayne R. Mantay

#### Design Considerations

The rotor dynamic design considerations are essentially limitations on the vibratory response of the blades which in turn limit the dynamic excitation of the fuselage by forces and moments transmitted to the hub. The following quantities associated with the blade response are subject to design constraints: blade frequencies, vertical and inplane hub shear, rolling and pitching moments, and aeroelastic stability margin.

Frequencies.- The blade natural frequencies are required to be separated from multiples of the rotor speed. A typical constraint is written as

$$\omega_{Li} \leq \omega_i \leq \omega_{ui} \quad (10)$$

where  $\omega_i$  is a blade frequency, and  $\omega_{Li}$ ,  $\omega_{ui}$  are lower and upper bounds of the  $i$ th frequency. Generally,  $\omega_{Li}$  and  $\omega_{ui}$  are  $n\Omega \pm \delta$  where  $n$  is an integer,  $\Omega$  is the rotor speed, and  $\delta$  is a tolerance usually about 10 percent of  $n\Omega$  (e.g., ref. 6).

Vertical hub shear.- The transmitted vertical hub shear  $S$  is to be made as small as possible. This requirement may be handled either as part of the objective function wherein it is minimized (ref. 6), or as a constraint where the vertical hub shear is required to be less than some specified value (ref. 23). In the first approach, letting  $N$  denote the number of blades in the rotor

$$|S_k| \rightarrow \min \quad k = N, 2N, \dots \quad (11)$$

In the second approach

$$|S_k| \leq \epsilon \quad k = N, 2N, \dots \quad (12)$$

where  $\epsilon$  is a positive value.

Only blade shear responses at multiples of  $N\Omega$  contribute to the transmitted vertical hub shear. The vertical blade shear at all other frequencies cancel out in the summation process. In other words

$$S_k \Big|_{\text{tot}} = \begin{cases} NS_k & k = N, 2N, \dots \\ 0 & \text{All other } k \end{cases} \quad (13)$$

At the same time, for a finite hinge offset, the blade vertical shear at other frequencies contributes to the transmitted hub moments.

Hub moments. - Two types of moments are generated at the hub due to blade motion. The first is due to distributed blade bending moments and the second is due to couples involving the blade shear forces at the hinge offset of the blade. Each type of moment has both a rolling and pitching component at the hub.

Inplane hub shear. - In the approaches described herein, the inplane hub shear is handled in the same way as the vertical hub shear. Specifically, in the first approach,

$$|H_k| \rightarrow \min \quad k = N, 2N, \dots \quad (14)$$

in the second approach

$$|H_k| \leq \epsilon \quad k = N, 2N, \dots \quad (15)$$

For an N-bladed rotor, the total transmitted shear at the hub is non-zero only at frequencies which are multiples of  $N\Omega$ . However, in this case, the transmitted hub shear is made up of contributions from the blade responses at the following multiples of the rotor speed:  $N \pm 1, 2N \pm 1, \dots$  For example, in a four-bladed rotor,

$$\left. \begin{aligned} X_4 &= (2F_5 - 2F_3) \cos 4\Omega t \\ Y_4 &= (2F_5 - 2F_3) \sin 4\Omega t \end{aligned} \right\} \quad (16)$$

where  $X_4$  and  $Y_4$  are orthogonal components of in-plane forces.  $F_3$  and  $F_5$  are amplitudes of tangential forces at the blade root at frequencies  $3\Omega$  and  $5\Omega$ , respectively. Thus  $X_4$  and  $Y_4$  play the roles of  $H_k$  in equations (14) and (15).

Rotor aeroelastic and aeromechanical stability.- The constraint for positive system aeromechanical stability relies on knowledge of fixed system characteristics and rotor frequency placement. Specifically, the rotor's lower modes, especially lead-lag, should not have fixed-system values which coalesce with the fuselage roll or pitch degrees of freedom, either on the ground or in flight.

Additionally, aeroelastic stability constraints for the isolated rotor in hover as developed by Friedmann (ref. 6) require that

$$\eta_k \leq \eta_{Lk} < 0 \quad (17)$$

where  $\eta_k$  is the real part of the kth complex eigenvalue and  $\eta_{Lk}$  is its limiting value.

#### Analysis Considerations

For the purpose of dynamic response analyses, the rotor blade is modeled as a beam undergoing coupled flap-lag-torsion motion in response to harmonically varying airloads. The beam is assumed to rotate at constant rotor speed which gives rise to centrifugal loading and stiffness effects. It is anticipated that either a finite-element analysis (e.g., ref. 24) or CAMRAD (ref. 14) will be used for the dynamic calculations. These calculations include mode shapes and (complex) eigenvalues, steady-state response (displacements), blade loads, and transmitted hub loads and moments.

The governing matrix equation for vibration response of a finite-element modeled structure is

$$M\ddot{X} + C\dot{X} + KX = F \quad (18)$$

where M is the mass matrix

C is the damping matrix

K is the stiffness matrix

X is the vector of displacements and rotations

F is the applied force vector

The stiffness matrix K for a rotor blade has the form

$$K = K_E + K_C + K_D$$

where  $K_E$  is the linear elastic stiffness matrix

$K_C$  is a centrifugal stiffness matrix

$K_D$  is the differential stiffness matrix and contains stresses associated with centrifugal forces

Detailed discussions and explicit forms for  $K_C$  and  $K_D$  are available in reference 24.

Equation (18) may be solved by modal superposition. The modal analysis produces the natural frequencies and damping needed in the phase 1 constraints (eqs. 10, 12, 15). Additional analyses are used to calculate the blade loads and transmitted hub loads based on modal expansions of the blade response and are outlined in reference 23.

Derivatives of the dynamic response quantities which appear in the constraints are needed. Expressions for most of these derivatives are given in reference 23. For example, analytical derivatives of the frequencies are given by

$$\frac{\partial \omega^2}{\partial v} = \phi^T \left( \frac{\partial K}{\partial v} - \omega^2 \frac{\partial M}{\partial v} \right) \phi \quad (19)$$

The alternative to finite-element analysis is the modified Galerkin approach in CAMRAD. The advantage of the latter approach is that it resides in the same code that will be used for the aerodynamic analysis. The disadvantage is that the method does not ordinarily generate the matrices M, C, and K which are needed for the analytical derivatives (e.g., eq. (19)). Thus, the modified Galerkin approach may require the use of finite difference derivatives. This was done in reference 7 without any ill effects. Nevertheless, studies are underway to find ways to generate equivalent M, C, and K matrices based on the modified Galerkin method and use these in the calculations of analytical derivatives.

ROTOR BLADE STRUCTURAL DESIGN

Mark W. Nixon

547812 P6  
N90-12584  
54-05  
220016  
61

In this section the structural design of rotor blades is discussed. The various topics associated with the structural design include constraints, load cases, and analyses.

Design Constraints

The constraints associated with traditional structural design can be categorized as aerodynamic, autorotation, buckling, frequency, and material strength. As discussed in reference 10, some of these constraints are based on maintaining characteristics required by other disciplines involved in the integrated optimization. Constraints associated with aerodynamics, autorotation and frequency are not addressed in this section, since they are addressed in other sections of the paper.

Of the remaining structural constraints, the most important is the material strength constraint. All stresses in the blade structure must be less than the design allowable stress of the material for all load cases. To account for stress interactions, a failure criterion such as Tsai-Hill (ref. 25) is calculated based on the material limit allowable stresses. The governing equation is

$$\bar{R} = \sqrt{\frac{\sigma_1^2}{X^2} - \frac{\sigma_1\sigma_2}{X^2} + \frac{\sigma_2^2}{Y^2} + \frac{\sigma_{12}^2}{S^2}} \quad (20)$$

The quantity  $(1 - \bar{R})$  is a margin of safety which must be greater than zero at all points of the blade. This constraint must be evaluated for several load cases which are discussed in detail in the Load Cases section.

A constraint is also applied for buckling of the blade spars. Buckling is not likely to occur when the blade system is rotating because of the high tensile loads induced by centrifugal forces. However, there are load conditions, discussed later in the Load Cases section, in which the blade is not rotating. In the absence of centrifugal forces, it is possible that buckling occurs at a stress below the allowable static stress. The buckling constraint is violated if the compressive stress due to bending exceeds a critical value which is given by reference 26 as

$$\sigma_c = K_c \frac{Et^2}{W^2} \quad (21)$$

for a D-shaped spar. In equation (21),  $E$  is Young's modulus,  $t$  is spar thickness,  $W$  is spar width, and  $K_c$  is a constant dependent on cross sectional geometry.

#### Load Cases

The static load cases used herein for structural optimization are outlined in reference 26, and are discussed in detail in reference 27. They are described below in terms of flapwise, inplane, torsional, centrifugal, and non-flight loads. The flapwise, inplane, torsional, and centrifugal loads are applied simultaneously. The non-flight loads are a separate case applied to the non-rotating cantilevered blade. The method of calculating the load magnitudes and distribution for each case are covered in this section.

Flapwise loads.- Flapwise load magnitudes are defined as a function of load factors,  $N_z$ , and the structural design gross weight of the total helicopter system, SDGW. The load factors are applied to account for the load increases which occur in maneuvers as well as appropriate factors of safety. The maneuver loads generally cannot be directly predicted with sufficient accuracy using current analysis techniques. The critical flapwise load factors used under current structural design requirements range from -0.5 to +3.5 for most military helicopters. The total flapwise load is equal to  $N_z$  times the structural design gross weight of the system. Thus, the magnitude of the flapwise load,  $L_f$ , carried by one blade in a rotor system of  $N$  blades is given by

$$L_f = (N_z)(SDGW)/N \quad (22)$$

Distribution of the load, which is a function of azimuthal position, should be representative of actual airloads the blade produces in steady level forward flight. The airloads include both steady and oscillatory parts, and are scaled proportionally at each spanwise segment until the total load (the sum of the load on each segment) equals the required load,  $L_f$ . The steady and oscillatory level flight blade airloads are obtained from an aerodynamic analysis using CAMRAD (ref. 14). The load distributions associated with several azimuthal positions will be considered. This increases the likelihood that all critical load distributions have been identified.

Inplane loads.- The inplane loads are based on two cases of shaft torque transmission from the powerplant. One case emanates from a power increase with subsequent rotor acceleration. Here, a shaft torque is transmitted through the hub creating an inplane moment at the blade root. The limit root inplane moment,  $M_E$ , is given by reference 26 as

$$N_E = \frac{1.5M_T}{N - 1} \quad (23)$$

where  $M_T$  is the torque developed at the military power rating of the powerplant. The second case requires that twice the maximum braking torque be equally transmitted to all blades. The root moment for both cases is balanced by an inertial force distribution developed along the blade span such that

$$M_E = \sum_{i=1}^n m_i r_i^2 \dot{\Omega} \quad (24)$$

where  $i$  refers to the  $i$ th blade segment of the beam model,  $m$  is segment mass and  $r$  is radial distance. After solving for  $\dot{\Omega}$ , the inplane inertial loads can be written as

$$q_i(r) = \frac{m_i r_i \dot{\Omega}}{l_i} \quad (25)$$

where  $l_i$  is the length of the  $i$ -th segment.

Torsional loads.- There are two basic contributions to the static torsional loads of a rotor blade. The first is due to the aerodynamic pitching moments on the airfoil sections which are obtained from the aerodynamic analysis. The second torsional load contribution is due to the inertial moments created by the centrifugal forces. Because rotor blades generally have a built-in twist, there will always be a part of the blade in which the inertial moments can be significant. The torsional loads produced here are proportional to centrifugal force, root angle of attack, and rotor twist such that

$$T_{PM_i} = I_{\theta_i} \Omega^2 \theta_i \quad (26)$$

where  $I_{\theta}$  is the moment of inertia about the blade axis, and  $\theta$  is the blade pitch angle.

Centrifugal loads.- Axial and flapwise components of centrifugal force in the  $i$ th blade segment  $(CF_i)_a$  and  $(CF_i)_f$ , are shown in figure 5. In the inplane load

case shown in figure 6, an inplane distributed inertial load,  $q(r)$ , creates a lag condition. Lead-lag rigid body displacements resulting from the inertial load do not create large opposing centrifugal force components because the centrifugal force vector acts nearly along the c.g. axis of the blade. The magnitude and distribution of the centrifugal load is governed by the equation

$$CF_i = m_i r_i \Omega^2 \quad (27)$$

where  $i$  refers to an individual blade segment of the beam model.

Non-flight loads.- The last load case covers aspects of non-flight loads. Reference 26 requires that an articulated rotor blade be designed for a static load equal to its weight multiplied by a limit load factor of 4.67. Reference 27 indicates that this load case can be used to cover other adverse conditions such as ground handling, stop-banging, turning the rotor at low speed in a strong wind, and the condition in which a helicopter with an untethered rotor is in the vicinity of an operating helicopter. For the non-flight load case, the blade is assumed to be cantilevered at the blade stops, and under no rotational effects. The non-flight load case is used to check for buckling of the blade spars.

#### Blade Structural Analyses

A choice must be made regarding the type of analytical model to use in the structural analysis. There are two analysis procedures which can give the detailed ply-by-ply stresses required to assess material strength margins of safety. One procedure is completely finite element based and uses a two-dimensional finite element model. The other procedure is a combination of a beam analysis (finite element or not) applied to a planform model and a laminate analysis applied to one or more cross section models. The two-dimensional finite element procedure requires significantly more computation time than the combination procedure. Time efficiency is very important when using a discipline-integrated optimization procedure because hundreds

ORIGINAL PAGE IS  
OF POOR QUALITY.

(possibly thousands) of analysis iterations are necessary. In preliminary design the accuracy of a combination of beam and laminate analyses is sufficient. Further, the superior efficiency with respect to computational time makes the combination procedure more desirable than the two-dimensional finite element procedure.

The combined beam and laminate analyses procedure requires two types of blade models: a beam model and a cross-section model. The beam model consists of a series of beam segments connected at spanwise grid points. Each segment contains equivalent beam properties such as the stiffnesses and masses. These properties are constant along a single beam segment, but may vary between segments, thus forming a step function of beam property distributions along the blade span. Displacements (translational and rotational) and beam forces (shears and moments) resulting from the applied loads are computed at the grid points.

A cross section model is a representation of the internal blade structure which is composed of several components. These components generally consist of one or more spars, a leading edge weight, an aft honeycomb or balsa core, and a skin. The cross section models serve two purposes. First, they are used to calculate the equivalent beam properties of the beam segments. Thus, there will be a different cross section model corresponding to each unique beam segment. Secondly, the cross section models are used to calculate stresses resulting from the forces associated with each beam segment. The stresses are then used in a laminate analysis to determine the margins of safety at various points in the cross section.

5717813 P6  
N90-12585  
5-05  
273 017

ACOUSTIC DESIGN CONSIDERATIONS

Ruth M. Martin

Review of Rotor Acoustic Sources

The acoustic signal from a helicopter rotor arises from several very complicated sources due to the aerodynamic loading of the blades, the interaction of the rotor with its wake, and the physical process of the blades moving through air. The

various sources can be quite different in their temporal character, have different frequency spectra, occur at different flight regimes, and have differing directivity patterns. One noise source may dominate the signal at a particular measurement location and flight condition while other sources may be important at a slightly different measurement location. Due to this diversity, it is not sufficient to optimize a rotor design in terms of a single noise level calculated for a single flight condition and a single measurement location. The various noise sources, their frequency content, amplitude, and directivity as a function of operating condition must be considered.

Rotor noise is often characterized in terms of its harmonic content and its broadband content. The harmonic content typically consists of the lowest multiples of the rotor blade passage frequency ( $f_{bp}$ , typically between 10 and 30 Hz). The low frequencies (the first 5 to 10 harmonics) are generally the highest in amplitude and have the greatest importance to military detection work. Some acoustic sources also create higher frequency harmonics of the  $f_{bp}$ . The broadband part typically occurs in the middle and higher frequency regions of the spectrum. The higher frequency content can be deterministic or random depending on flight conditions, and is the most important for community noise problems and aircraft noise certification, since aircraft certification measurements emphasize the middle frequencies.

The following paragraphs present a summary of the frequency ranges, directivity patterns and the most important operational and design parameters for each major rotor noise source. Figure 7 shows the frequency ranges of these noise sources, and figure 8 shows their general directivity patterns.

Loading noise is due to the low frequency time varying lift on the blades and is a strong function of the local lift distribution ( $C_l$ ) and rotor thrust coefficient ( $C_t$ ). This source may be predicted from the measured or predicted blade surface pressure distribution. It is the predominant contributor to the low frequency

content (1 to 10  $f_{bp}$ ) at moderate advance ratios ( $\mu$  up to 0.3). Analysis has shown that the strongest radiation direction is down from the rotor plane.

Thickness noise is due to the motion of the blades through air and is a strong function of blade thickness and local Mach number. This source may be predicted from a definition of the blade geometry and the rotor motion. It is a dominant contributor to the low frequency content (1 to 10  $f_{bp}$ ) at the higher advance ratios ( $\mu$  above 0.3). Analysis and experimental data have shown that its strongest radiation direction is in the plane of the rotor.

High speed impulsive noise (HSI) occurs when high transonic local Mach numbers occur on the advancing-side tip region. The result is a strong increase in the low frequency harmonics (1 to 20  $f_{bp}$ ) and a steepening negative pulse in the noise signal. This source is very sensitive to tip Mach number and blade shape, particularly in the tip region. The directivity pattern of HSI is similar to that of thickness noise, strongest in the rotor plane. Although observed experimentally, due to nonlinear transonic effects, this source is not as well predicted as the subsonic loading and thickness noise.

Blade-vortex interaction noise (BVI) is attributed to the aerodynamic interaction of the trailing tip-vortices with the following blades, and is essentially a higher frequency loading noise. The BVI impulsive signal consists of higher harmonics and subharmonics of the  $f_{bp}$ , typically in the range of 5 to 30  $f_{bp}$  harmonics, and occurs mostly at low advance ratios (0.1 to 0.2) in descent. When this source is generated it dominates the midfrequencies of the acoustic spectrum. The directivity is generally out-of-plane as is low frequency loading noise, but is more focused in its primary radiation direction. This acoustic source can be calculated in the same manner as low frequency loading noise but the results depend heavily on the accuracy and resolution of the aerodynamic prediction.

Broadband rotor noise is a very general term for several non-periodic aerodynamic noise sources primarily due to atmospheric turbulence and blade self-generated

turbulence. Broadband noise is affected by changes in boundary layer characteristics, so tip speed, blade shape and Reynolds number effects are important. Although broadband noise levels are significantly lower than the other rotor noise sources, this source is the main contributor to the high frequencies (above  $25 f_{bp}$ ). The directivity is thought to be a dipole pattern aligned with the rotor axis. The prediction of this noise source is not as mature as the more deterministic rotor noise sources and is currently under development.

### Acoustic Design Requirements

Phase 1 of the optimization approach will not include an acoustic analysis coupled with the optimization process. Instead, the acoustic aspects of the problem will be accounted for in terms of effective acoustic design requirements. It is difficult to generalize design requirements for rotor noise because the acoustic output varies so widely depending on the noise source, flight condition, measurement location, and frequency range. However, assuming the rotor must lift a fixed nominal payload and operate over a wide range of flight conditions, three general design guidelines can be stated: (1) minimize tip Mach number, (2) minimize blade thickness in the tip region, and (3) minimize gradients in the spanwise lift distribution in the tip region. The first two guidelines are aimed at minimizing thickness noise and high speed impulsive noise. The third guideline is aimed at minimizing the tip vortex strength, and thus blade-vortex interaction noise.

For the phase 1 approach, constraints on blade thickness, maximum values for hover tip mach number ( $M_{tip}$ ), advancing tip Mach number ( $M_{1,90}$ ) and spanwise lift coefficient gradient ( $\partial C_l / \partial (r/R)$ ) will be specified during the aerodynamic, dynamic and structural optimization process (table 2).

### Acoustic Evaluation of Rotor Designs

Once a rotor design has been optimized for the aerodynamic, dynamic, and structural constraints, including the acoustic design requirements, it will be input to an

acoustic analysis for evaluation. In addition, perturbed designs will be provided, designs for which each of the design variables have been perturbed from the optimum design value. The acoustic analysis will calculate the acoustic output of the nominal and perturbed designs. Derivatives of the acoustic output with respect to the design variables will then be calculated to identify the most important acoustic parameters.

The rotor noise sources to be considered in the phase 1 analysis include the low frequency loading and thickness noise, and the higher frequency noise due to blade-vortex interactions (BVI). Broadband and high speed impulsive noise will not be addressed in phase I, but may be included in phase 2 or 3. The analyses to be employed will include the comprehensive rotor analysis and design program CAMRAD (ref. 14) and the rotor noise prediction program WOPWOP (ref. 28). The acoustic analysis will calculate three integrated sound pressure levels to quantify (1) the low frequency acoustic content, (2) the mid frequency acoustic content, and (3) the A-weighted sound pressure level, a common noise metric used in aircraft certification procedures. The acoustic signal will be predicted for several measurement locations where the different noise sources are important, for the flight conditions considered in the objective function (see eq. 1).

#### Basis of Acoustics Analysis

The problem of rotor noise prediction can be represented as the solution of the wave equation if the distributions of sources both on the moving surface (the rotor blade) and in the flow are known. Ffowcs Williams and Hawkins (ref. 29) derived the governing differential equation by applying the acoustic analogy of Lighthill (ref. 30) to bodies in motion. Subsequently, Farassat developed several integral representations of solution of the Ffowcs Williams-Hawkings (FW-H) equation that are valid for general motions in both subsonic and supersonic flow (refs. 31-33).

The acoustics analysis (ref. 28) is based on dividing the rotor blade surface into a number of panels. Appropriate numerical integrations are carried out using the integrand value at the panel center for the entire panel area. The program determines the panel center and calculates the contribution to the noise from the panel for a specified number of times (azimuth angles). This is repeated for each blade and for all panels to complete the integration over the blade surface.

The program requires a namelist input and three input subroutines. The namelist provides the flight conditions and program control parameters. The subroutines describe the physical and aerodynamic characteristics of the rotor blade and allow great flexibility in the definition of the blade geometry and loading. One subroutine defines the blade-section geometric twist, chord, pitch change axis location, maximum thickness ratio and maximum camber ratio as a function of radial position along the rotor blade. A second subroutine defines the camber and thickness as functions of radial and chordwise locations. The third subroutine describes the aerodynamic blade loading on either the actual blade surface or the mean camber surface as a function of azimuthal position. The blade loading input will be provided by the output of the CAMRAD calculations for all flight conditions, for each of the rotor designs to be evaluated.

547814 Ry.  
N90-12586

56-05

220013

48.

AIRFRAME DESIGN CONSIDERATIONS

Raymond G. Kvaternik and T. Sreekanta Murthy

Overview

The purpose of this section of the paper is to provide a discussion of those aspects of airframe structural dynamics that have a strong influence on rotor design optimization. Primary emphasis is on vibration requirements. The constraints imposed on rotor design by airframe dynamics and included in Table 2, are discussed.

The section also includes a description of rotor/airframe modeling enhancements which may be incorporated in later phases of this work.

#### Constraints Imposed by Airframe on Rotor Design

The design of a rotor which, when coupled to an existing airframe, will result in minimum vibration levels in the airframe requires knowledge of the latter's dynamic characteristics. Because the airframe design is fixed, it is assumed that its dynamic description in terms of both its frequency response characteristics and its frequencies, mode shapes, and modal structural damping are known. It is also assumed that the airframe hub impedance can be computed for the excitation frequencies of interest (which depend on the number of blades and the rotor rotational speed).

Constraints due to vibration response. - To insure that the vibratory responses of the airframe are at minimum levels requires: (1) insuring that none of the frequencies of the major airframe modes is close to the predominant transmitted rotor exciting frequencies; and (2) minimizing the rotor induced loads which are transmitted to the airframe.

The proximity of airframe modes to a rotor exciting frequency as well as an indication of the vibratory response levels under excitation are usually determined by inspection of frequency response functions which are computed (or measured) for the airframe structure. Frequency response curves typically have the form depicted in figure 9, which shows the airframe response (usually the acceleration in g's) at some point (and direction) as a function of hub excitation frequency. Usually, many curves of this kind are generated corresponding to each unique combination of the type (force or moment) and direction (vertical, lateral, etc.) of excitation and the response points and directions of interest. The peaks on the curve occur at the natural frequencies of the airframe; the higher peaks correspond to modes which are major contributors to the total response. The valleys represent low levels of response. As previously mentioned, the oscillatory loads transmitted from the rotor to

the airframe occur at integer multiples of  $N\Omega$  (where  $N$  is the number of blades). Because the magnitude of these loads decreases with increasing harmonic number, usually only  $N\Omega$  (and sometimes  $2N\Omega$ ) need be considered in practice. Now the number of blades and the rotor rotational speed are generally dictated by aerodynamic requirements. Usual practice is to design the airframe to avoid frequency placement which would result in either resonance or high amplification at  $N\Omega$  (and perhaps  $2N\Omega$ ). Because the airframe structural design is assumed to be fixed in phase I of the current work, the design requirement necessitated here is to select  $N$  and  $\Omega$  such that the rotor excitation frequencies  $N\Omega$  and  $2N\Omega$  are sufficiently removed from the frequencies of the major airframe modes.

Aeromechanical stability constraints.- Aeromechanical instabilities are phenomena in which the inertial coupling between the motion of the first inplane blade mode and any airframe mode that involves hub motion in the plane of the rotor produces a growing oscillation. This may occur on the ground (ground resonance) or in flight (air resonance) (refs. 34 and 35).

Assessment of both ground and air resonance can be made from plots of the type shown in figure 10, which show the variation with rotational speed of the pertinent airframe and rotor mode frequencies, both expressed with respect to the nonrotating system. For simplicity, the uncoupled system frequencies are shown in figure 10. The open circles denote points of frequency coalescence between the critical rotor mode and an airframe frequency and are regions of potential instability. The rotor design requirement to avoid instabilities is to insure that, within the operating speed range of the rotor, there are no coincidences of the frequency of the critical rotor mode with an airframe mode.

#### Future Design Role of Rotor/Airframe Coupling

It has long been recognized that the dynamic (and aerodynamic) interaction of the rotor and the airframe is important in analysis of helicopter vibrations.

However, the complexity of the problem has been so overwhelming that it has long been customary to compute the blade (and hence rotor) vibratory loads assuming that the hub is fixed. These loads are then applied to separate analytical models of the rotor and the airframe for determining their respective responses. It is clear that this approach cannot entirely account for the interactions between the rotor and the airframe. A simplified view of how the rotor and the airframe interact to produce vibrations is depicted in figure 11. The airframe motions caused by blade response excite the hub to vibrate which alters the aerodynamic loading on the blades and hence the loads transmitted back to the airframe. Depending on the type and configuration of the hub, this interaction can substantially affect the loads which act both on the rotor and on the airframe (ref. 36).

Among the practical methods for calculating the vibrations of a helicopter as a single system, those methods that are based on impedance matching techniques which effect a solution in the frequency domain rather than in the time domain appear to be better suited for use in design work. While impedance methods have been known to the helicopter community for many years and have been employed in analysis of helicopter vibrations (see, for example, refs. 37-39), they have not been used extensively in design to limit vibrations. A rotor impedance matrix can be generated to represent a correction to the gross rotor vibratory forces resulting from small displacements of the rotor from equilibrium during trimmed flight conditions. Compatibility conditions between the hub and airframe lead to "harmonic balance" equations. This set of simultaneous linear algebraic equations are solved for the hub motions, from which the more accurate airframe (and rotor) vibrations are computed. Although not included in the phase 1 activity, the above modeling improvement is planned for incorporation in phases 2 and 3.

547815 P7  
N90-12587

ORIGINAL PAGE IS  
OF POOR QUALITY

VALIDATION OF THE PROCEDURES

Wayne R. Mantay

220019  
73

Approach

Assessing the fidelity of a complex system or analysis in a comprehensive manner is always an ambitious task. Validation of the same system, while providing objective proof of concept, increases the difficulty of the job by requiring all subsystems to be verified. Design methodology, especially for rotorcraft, needs a comprehensive validation procedure because of the interdisciplinary nature of the system. Both tool validation of the individual disciplines and proof-of-design for the entire system must be addressed. A primary goal of this activity is the comprehensive validation of all critical steps in the design integration process.

The ability to synthesize a design depends, to a large extent, on the correct prediction of critical phenomena. For a rotor system design which includes performance, dynamics and structural goals, the aeroelastic characteristics of the blade and stresses (for example) would be critical to know. Once the prediction fidelity of the rotor's phenomenological events is proven, parametric sensitivity of these design tools must be examined, since obtaining a global design will depend on quantifying the effects of controlled changes about some initial design.

Also of interest for rotor design validation is the evaluation of techniques for modifying a design. Techniques for changing performance, vibratory loads and material properties in a controlled way become invaluable design tools, but only if their consistency has been proven. Such techniques might include structural tailoring, modal alteration, and airfoil and planform variations.

Following the assessment of these design building blocks, their integration must be evaluated. For this to be an objective measure of rotor design performance, several conditions should be met. The rotor task and mission for the optimized rotor system should not be beyond the range of validity for which the phenomenological building blocks were assessed. Furthermore, the baseline rotor system should be one

which satisfies most of the design constraints and for which descriptive data are available.

The goal of the first phase of this project is to design and validate a rotor system which accomplishes a challenging mission and task. One candidate set of mission specifications is given in table 4.

The sequence of validation will focus on the verification of the integrated design system and both optimized and baseline rotor designs in model and full scale. In the process, the concurrent assessment of the critical phenomena analyses and modifying techniques will be made.

#### Sequence of Test Problems

As already mentioned, the analyses used herein for aerodynamics, dynamics, structures, and acoustics prediction are, respectively, CAMRAD (ref. 14), a finite element code or CAMRAD, Coupled Beam Analysis (ref. 10), and WOPWOP (ref. 28). Each of these analyses provide information which can be used to predict design performance and design sensitivity. Several tests are ongoing or planned to evaluate the input requirements for these modules as well as the accuracy of the individual modules. The investigations of these tools range from those which are basic to rotor design but are not highly sensitive to small perturbations in the design, to those techniques which, in fact, could drive primary design variables. Some examples follow.

Validating the basic rotor environment prediction tools.- The local rotor inflow drives the rotor's performance, loads and acoustic characteristics. Prediction of this primary phenomenon has been elusive (ref. 40). A comprehensive mapping of this important parameter has been accomplished at the Langley Research Center by a significant investment in materiel and personnel. Although the mean flow may not be highly sensitive to small rotor changes, there are indications that prime variables measurably affect both the mean and time dependent inflow velocity field. Global

codes which are design coupled need this information if basic design decisions are to be effected in an automated manner.

Another key rotor phenomenon which drives airloading and hence, acoustic design constraints, is blade vortex interaction (BVI). The WOPWOP code can predict this high frequency noise source as well as the low frequency loading and thickness noise harmonics. How well the BVI prediction can be made depends on the quality of the aerodynamic input. Proving the fidelity of this acoustic source prediction relies heavily on experiments designed to specifically probe this area of fluid mechanics (ref. 41).

Structural mechanics is a strong design driver and couples with other disciplines in all phases of the plan. Even as a separate discipline it can provide innovative structural concepts for rotors, but those predicted characteristics need to be proven if advantage is to be taken of them by, for example, aerodynamic design requirements. A series of experiments to explore the predictability and parametric sensitivity of composite couplings is underway (ref. 42). The ability to design and build a rotor blade structure which is efficiently strong for steady and oscillatory loads and which also provides useful couplings for rotor performance, dynamics and stability enhancement is the goal.

Rotor aerodynamic design usually includes multimission requirements. Even a point design must hover and transition to forward flight. The ability of aerodynamic codes to predict the performance sensitivity of geometric design variables is a controversial issue. A parametric study has been undertaken (ref. 43) to assess the rotor's performance variability with controlled geometric changes, while all other variables are held constant.

Higher order validation of the prediction tools. - The coupling of rotor aerodynamics, dynamics, and structures is, of course, the challenge which this design procedure faces. The phenomenological building blocks just mentioned must be

combined in a systematic manner, the success of which is traceable. Several multidisciplinary studies are ongoing to accomplish this.

An improved design for the UH-60 Growth BLACK HAWK rotor (ref. 22) achieved its performance goals but incurred generally higher blade loads. A brief attempt at passive dynamic tuning using a modal shaping technique resulted in both unchanged and improved designs, depending on the numerical model used to predict the best location for nonstructural mass. In order to more fully explore the coupled aerodynamic/dynamic design drivers, model blades with spanwise variable nonstructural mass inside an advanced blade have been prepared for tests in the Langley Transonic Dynamics Tunnel (TDT). These model blades (denoted GBH-T) will also be available to validate the dynamic optimization procedures described previously.

Large changes in rotor rpm have historically been avoided in the operation of modern helicopters. As previously mentioned, the effect of rotational speed on most design disciplines is large. In order to use that variable in a design, the coupling effects between disciplines must be well known. The Aerodynamically and Dynamically Advanced Multi-Speed (ADAM) Rotor project (ref. 44) is currently exploring both the performance and dynamic opportunities and challenges of large rotor rpm variations.

Blade-to-blade variability, well known for its effect on vibration, also influences performance and acoustics (ref. 45). The use of this alteration of rotor state is unpredictable by most of today's global codes since they either assume perfect blade track, or the parameter sensitivities which create a maverick blade are not well-known. In order to address the latter problem, a series of representative aerodynamic blades with parametric internal changes are soon to be tested at Langley for out-of-track response to single blade inertial, elastic, controls and aerodynamic perturbations. Once the response of a blade to these changes becomes predictable, another "degree-of-freedom" will be possible for the designer and, ultimately, for an optimization procedure.

Validation of an overall rotor design.- In addition to testing the fidelity of the individual prediction tools, the final design of the rotor system must be verified in terms of satisfaction of design constraints and minimization of the objective function. First, experimentally verifying the satisfaction of the design constraints can be achieved in several ways. One way is a scale model test of both baseline and optimized rotors in an environment which simulates the imposed mission while affording a minimum of test "excuses." The model rotor should be at least 1/5 geometric scale and fully Mach scaled, with dynamic similarity. The wind tunnel and model fixed system should be chosen to provide a measure of constraint matching for acoustics and stand frequency avoidance. Following this with a full-scale test of the same configurations would enhance the design's credibility.

Second, assuring minimization of the objective function, is more difficult. Not only does the advanced rotor need to perform better than the baseline in the areas of aerodynamics, vibration, and acoustics, but a determination of minima must be made. This will, in all likelihood, involve perturbation of the advanced rotor's state and characteristics in the neighborhood of the predicted optimum design. Such a process is laborious and hardware intensive. It is envisioned that the parametric variations on this advanced model rotor will be guided by the validation of the predictive tools. Again, a full-scale test of the rotor design, with results compared to the baseline, would be ideal. Considering the minimization of objective functions, the full-scale article should have some variability also, and this will be guided by the model test results.

#### SCHEDULE AND MILESTONES

The near term schedule and milestones for the integrated optimization procedure are shown in Figure 12. This schedule goes through the completion of phase 1 including the design, fabrication, and testing of the rotor test article which will be used to validate the overall phase 1 procedure. The schedule also includes the

completion of the phase 2 development and a significant portion of phase 3. All of the items in the milestones have been mentioned in the paper to some extent.

There is a certain amount of overlap among the phases. For example, the formulations of the phase 2 and phase 3 optimization problems take place during phase 1. The development of acoustic sensitivity analysis and airframe dynamic sensitivity analysis which are needed for phases 2 and 3 respectively are to be initiated during phase 1. This overlapping is essential in the case of the sensitivity analyses since they are long lead-time developments and represent ground-breaking research.

It is again emphasized that validation is a continuing and crucial feature of the work as evidenced by a validation line in the schedule. Although the validation line is contained within the phase 1 portion of the figure, it is understood that validation of the procedures is a continuing activity beginning with the initial optimization development step of each phase, through the analytical/test comparisons for the test article which will certify the overall procedure.

#### CONCLUDING REMARKS

This paper has described a joint activity involving NASA and Army researchers at the NASA Langley Research Center to develop optimization procedures aimed at improving the rotor blade design process by integrating appropriate disciplines and accounting for all of the important interactions among the disciplines. The disciplines involved include rotor aerodynamics, rotor dynamics, rotor structures, airframe dynamics, and acoustics. The work is focused on combining the five key disciplines listed above in an optimization procedure capable of designing a rotor system to satisfy multidisciplinary design requirements.

Fundamental to the plan is a three-phased approach. In phase 1, the disciplines of blade dynamics, blade aerodynamics, and blade structure will be closely coupled, while acoustics and airframe dynamics will be decoupled and be accounted for as effective constraints on the design for the first three disciplines. In phase 2,

acoustics is to be integrated with the first three disciplines. Finally, in phase 3, airframe dynamics will be fully integrated with the other four disciplines. This paper dealt with details of the phase 1 approach. The paper included: details of the optimization formulation, design variables, constraints, and objective function, as well as details of discipline interactions, analysis methods, and methods for validating the procedure. Three sections of the paper deal with the individual disciplines of rotor aerodynamics, rotor dynamics, and rotor structures. In each section, the appropriate design constraints, design variables, and analytical details for computing appropriate responses are described. Two sections of the paper describe how the acoustics and airframe dynamics behaviors are incorporated as constraints into the design procedure. For example, acoustics imposes a local Mach number constraint on the blade velocity and angle of attack; and airframe dynamics imposes constraints on the rotor blade natural frequencies to avoid ground resonance through coalescence of blade and airframe frequencies. The plan for validating the components of the design process was described and the strategy for overall validation of the design methodology was defined. These validations are viewed as critical to the success of the activity and are viewed as the primary products of the work. Finally, some representative results from work performed to date are shown in the appendix. These include aerodynamic optimization results for performance, dynamic optimization results for frequency placement, optimal placement of tuning mass for reduction of blade shear forces, and blade structural optimization for weight minimization subject to strength constraints.

58-05-547816 P41  
22-90-12588

APPENDIX - RESULTS OBTAINED TO DATE

Joanne L. Walsh, Aditi Chattopadhyay,  
Jocelyn I. Pritchard, and Mark W. Nixon

To date, progress has been made in the areas of aerodynamic performance optimization, dynamic optimization, optimum placement of tuning masses for vibration reduction, and structural optimization. Selected results from these activities are highlighted in this appendix.

Results - Aerodynamic Performance Optimization

This section of the paper describes the application of formal mathematical programming to optimization of the aerodynamic performance of rotor blades. This work is described in detail in reference 9.

A previous analytical procedure for designing rotor blades, referred to herein as the conventional approach (ref. 46) served as the starting point for the development of the method in reference 9. The method of reference 46 combined a momentum strip theory analysis for hover (HOVT) based on reference 17 and the Rotorcraft Flight Simulation computer program (C-81, ref. 47) for forward flight. The program HOVT was used to compute hover horsepower. The program, C-81, (quasi-static trim option) was used to define the trim condition, the horsepower required, and the airfoil section drag coefficients for forward flight and maneuver conditions. Both analyses used experimental two-dimensional airfoil data.

The mathematical optimization formulation in reference 9 can be stated in terms of a design goal and a set of design requirements. The design goal is to reduce the hover horsepower for a given helicopter with a specified design gross weight operating at a specified altitude and temperature. Satisfactory forward flight performance is defined by the following three requirements. First, the required horsepower must be less than the available horsepower. Second, airfoil section stall along the rotor blade must be avoided, i.e., the airfoil sections distributed along the rotor blade

must operate at section drag coefficients less than a specified value neglecting the large drag coefficients in the reverse flow region. Third, the helicopter must be able to sustain a simulated pull-up maneuver, i.e., the aircraft must operate trimmed at a gross weight equal to a specified multiple (load factor) of the design gross weight for a second specified horizontal velocity  $V_{1f}$ .

In reference 9, the airfoil selection and distribution were preassigned. The design parameters point of taper initiation, root chord, taper ratio, and maximum twist - are illustrated in figure 13. The point of taper initiation,  $r$ , is the radial station where taper begins. The blade is rectangular up to this station and then tapered linearly to the tip. The taper ratio,  $TR$ , is  $c_r/c_t$  where  $c_r$  is the root chord and  $c_t$  is the tip chord. The twist varies linearly from the root to the tip where the maximum value  $\tau_{max}$  occurs. The approach uses the same rotor blade performance analyses as reference 46, but couples a general-purpose optimization program to the analyses. Using this approach, the user is less involved in manipulating the design variables as he would be using the conventional approach. Instead, the optimization program takes over the role of manipulating the design variables to arrive at the best blade design.

In reference 9 the mathematical programming approach was used to obtain rotor blade designs for three Army helicopters - the AH-64, the UH-1, and a conceptual high-speed performance helicopter. In each case the goal was to find, for preselected rotor speed, rotor blade radius, airfoil sections and distribution, the blade configuration which has the lowest hover horsepower for a given design gross weight and a selected pull-up maneuver. Results obtained in references 9 and 44 for the AH-64 helicopter are presented here.

The final AH-64 rotor blade designs obtained using both the conventional and mathematical programming approaches are shown in figure 14. Results include the final design variable values, the main rotor horsepowers required for hover (the objective function), for forward flight, and for the simulated pull-up maneuver

conditions, for each approach. The mathematical programming approach produces a design which had more twist, a point of taper initiation further outboard, and a smaller blade root chord than the conventional approach. The mathematical programming design requires 25 fewer horsepower in hover than the conventional design. Most significantly, mathematical programming approach obtained results about 10 times faster than the conventional approach (2 days vs. 5 weeks).

#### Results - Dynamic Optimization Through Frequency Placement

One important dynamics design technique is to separate the natural frequencies of the blade from the harmonics of the airloads to avoid resonance. This can be done by a proper tailoring of the blade stiffness and mass distributions. This section of the paper describes a procedure developed in reference 7.

Minimum weight designs of helicopter rotor blades with both rectangular and tapered planforms have been obtained subject to the following constraints: (a) upper and lower bounds ("windows") on the frequencies of the first three elastic lead-lag dominated modes and the first two elastic flapping dominated modes, (b) minimum prescribed value of blade autorotational inertia, and (c) upper limit on the blade centrifugal stress. Side constraints have been imposed on the design variables to avoid impractical solutions.

Design variables (fig. 15) include blade taper ratio, dimensions of the box beam located inside the airfoil section, and magnitudes of the nonstructural masses. The program CAMRAD has been used for the blade modal analysis and the program CONMIN has been used for the optimization. In addition, a linear approximation involving Taylor series expansion has been used to reduce the analysis effort. The procedure contains a sensitivity analysis which produces analytical derivatives of the objective function, the autorotational inertia constraint, and the stress constraints. A central finite difference scheme has been used for the derivatives of the frequency constraints.

The optimization process begins with an arbitrary set of design variable values. The mathematical formulation of the optimization problem is presented in figure 16. The blade weight  $W$  has two components  $W_b$  (structural weight) and  $W_o$  (nonstructural weight) and is expressed in the discretized form in figure 16, where  $N$  denotes the total number of segments and  $\rho_j$ ,  $A_j$ ,  $L_j$ , and  $W_{o_j}$  denote the density, the cross sectional area, the length, and the nonstructural weight of the  $j$ th segment, respectively. The subscripts  $L$  and  $U$  refer to the respective lower and upper bounds,  $\sigma_k$  is the centrifugal stress in the  $k$ th segment,  $M_j$  is the total mass of the  $j$ th segment, and  $\Omega$  is the blade rpm. The quantity  $FS$  denotes a factor of safety and  $\sigma_{max}$  is the maximum allowable blade stress.

The reference blade (refs. 5 and 7) shown in figure 15 is articulated and has a rigid hub. The blade has a rectangular planform, a pretwist, and a root spring which allows torsional motion. A box beam with unequal vertical wall thicknesses is located inside the airfoil. As in reference 5, it is assumed that only the box beam contributes to the blade stiffness, that is, contributions of the skin, honeycomb, etc. to the blade stiffness are neglected. For the rectangular blade, the box beam is modeled by ten segments and is uniform along the blade span. For the tapered blade, the box beam is tapered and is modeled by ten segments. A linear variation of the box beam height,  $h$ , in the spanwise direction has been assumed.

Table 5 presents a summary of the optimization results for the rectangular blade with 30 design variables (three box beam dimensions at ten segments) and the tapered blade with 42 design variables (30 box beam dimensions, 10 segment masses, taper ratio, and root chord). The optimum rectangular blade is 2.67 percent lighter than the reference blade and the optimum tapered blade is 6.21 percent lighter than the reference blade. The optimum tapered blade has a taper ratio ( $\lambda_h$ ) of 1.49. The first lead-lag frequency ( $f_1$ ) is at its prescribed upper bound after optimization and the autorotational inertia is at its lower bound for all cases. Additional results along with optimum design variable distributions can be found in reference 7 which

also discusses the effect of higher frequency constraints and stress constraints on the optimum blade weight and design variable distributions.

#### Results - Optimum Locations of Vibration Tuning Masses

The objective of this work is to develop and demonstrate a method for optimally locating, as well as sizing, tuning masses to reduce vibration using formal mathematical optimization techniques. The design goal is to find the best combination of tuning masses and their locations to minimize blade root vertical shear without a large mass penalty. The method is to formulate and solve an optimization problem in which the tuning masses and their locations are design variables that minimize a combination of vertical shear and the added mass with constraints on frequencies to avoid resonance. Figure 17 shows an arbitrary number of masses placed along the blade span. Two alternate optimization strategies have been developed and demonstrated. The first is based on minimizing the amplitudes of the harmonic shear corresponding to several blade modes. The second strategy reduces the total shear as a function of time during a revolution of the blade. Results are shown in which the above strategies are applied to a rotor blade considering multiple blade mode/multiple harmonic airload cases.

The example problem is a beam representation of an articulated rotor blade. The beam is 193 inches long with a hinged end condition and is modeled by 10 finite elements of equal length. The model contains both structural mass and lumped (non-structural) masses. Three lumped masses are to be placed along the length of the beam. The first strategy was applied to minimize the 4/rev blade root vertical shear response  $S_4$  of the first and second elastic flapping modes without using excessive tuning mass. Figure 18 summarizes the initial and final designs. The initial shear amplitude is 34.68 lbf which is reduced by the optimization process to 0.01 lbf with an accompanying decrease in the tuning mass. The second strategy was applied to a test case of two modes responding to three harmonics of airload. Figure 19 shows for

the initial and final designs, the shear  $s(t)$  plotted as a function of the time and azimuth for a revolution of the blade. The peaks on the initial curve have been reduced dramatically. For example, the maximum peak  $s_{\max}$  for the initial design is 78.00 lbf, and for the final design, the maximum peak is 0.576 lbf.

#### Results - Rotor Structural Optimization

A blade structural optimization procedure (fig. 20) applicable to metal and composite blades has been developed in which the objective function is blade mass with constraints on frequencies, stresses in the spars and in the skin, twist deformation, and autorotational inertia. The design variables are the total spar thickness and for the composite blade the percentage of  $\pm 45^\circ$  plies (the remaining plies assumed to be at  $0^\circ$ ). This procedure is described in detail in reference 10, and additional applications of the methods are also given in reference 10.

This section describes two example rotor blade designs which were developed using the structural design methodology. Both designs are based on the UH-60 Black Hawk titanium spar blade. The first design case is for a titanium single spar cross section. This design was conducted to validate the present design methodology. The second case has a graphite/epoxy spar in a single spar cross-section configuration. The composite spar design is compared to the metal spar design to explore potential weight savings obtained from use of the design methodology in conjunction with composite materials.

Titanium cross section. - A titanium spar blade design was developed using the previously described design methodology. The cross-section model was based on the UH-60 rotor blade with identical skin, core, trailing edge tab, leading edge weight, and spar coordinates. Only the spar thickness was used as a design variable. The beam model representation of the blade used a rectangular planform similar to the UH-60 planform, but without any tip sweep. A maximum twist of deformation of  $3.1^\circ$  is based on an aerodynamic performance constraint (ref. 10). The structural constraint

requires that the calculated stresses do not exceed the allowable material strength. The material strength is assessed by use of a Tsai-Hill failure criterion based on the associated margins of safety. The margins of safety must be greater than zero to satisfy the material strength constraint. The autorotation capability is assumed to be the same for this design as it is for the UH-60. Autorotation is satisfied by requiring the mass moment of inertia to be identical to that of the UH-60 rotor system which is 19000 in-lbs-s per blade. Before a comparison to the UH-60 blade can be made, the design must be dynamically tuned. The modes considered in this design are first elastic flapwise and edgewise bending, first torsion, and second and third flapwise bending. The frequencies of these modes are required to be removed from integer multiples of the forcing frequency by 0.2 per rev.

As shown in figure 21, the minimum spar thickness needed to satisfy all the constraints is 0.130 inch which corresponds to a blade weight of 207 pounds. The actual UH-60 titanium spar is 0.135 inch thick, producing a 210 pound blade. The titanium spar design is only 3 pounds different from the actual UH-60 blade, demonstrating that the mechanics of the design methodology can produce blade designs similar to conventional design processes. The only significant difference in modal frequencies between the actual UH-60 blade and the titanium spar design is the frequency of the torsional mode. The difference is attributed to the chordwise distribution of the nonstructural tip weight which, in the present titanium spar design, was lumped at the chordwise c.g.

Composite cross section.- A second design was developed using a single T300-5208 graphite/epoxy D-spar. The blade models and associated design assumptions used in the composite design were the same as those used for the metal spar except for the spar material. Here, thickness and ply orientation of the composite spar were used as design variables. The plies of the spar were assumed to consist only of  $0^\circ$  and  $\pm 45^\circ$  angles symmetrically built up. Thus, the ply orientation design variable was the percentage of  $\pm 45^\circ$  plies in the laminate. The remaining plies of the laminate

are understood to be oriented at  $0^\circ$ . Constraints on twist deformation, material strength, mass moment of inertia, and dynamic tuning are the same as those used for the metal design.

Results shown in figure 21 show that the composite design satisfied the required constraints. Further, the minimum weight design had a 0.105 inch thick spar with 20 percent of the plies oriented at  $\pm 45^\circ$  degrees which resulted in blade weight savings of 21.5 percent. These results demonstrate that this design methodology, used in conjunction with composite materials, can result in significant weight savings.

## REFERENCES

1. Ashley, H.: On Making Things the Best - Aeronautical Use of Optimization. AIAA Journal of Aircraft, vol. 19, no. 1, 1982.
2. Sobieszczanski-Sobieski, J.: Structural Optimization Challenges and Opportunities. Presented at International Conference on Modern Vehicle Design Analysis, London, England, June 1983.
3. Miura, H.: Application of Numerical Optimization Methods to Helicopter Design Problems: A Survey. NASA TM-86010, October 1984.
4. Bennett, R. L.: Application of Optimization Methods to Rotor Design Problems. Vertica, vol. 7, no.3, 1983, pp. 201-208.
5. Peters, D. A.; Rossow, M. P.; Korn, A.; and Ko, T.: Design of Helicopter Rotor Blades for Optimum Dynamic Characteristics. Computers and Mathematics With Applications, vol. 12A, no. 1, 1986, pp. 85-109.
6. Friedmann, P.: Application of Modern Structural Optimization to Vibration Reduction in Rotorcraft. Vertica, vol. 9, no. 4, 1986, pp. 363-376.
7. Chattopadhyay, Aditi; and Walsh, Joanne L.: Minimum Weight Design of Rotorcraft Blades With Multiple Frequency and Stress Constraints. Proceedings of the AIAA/ASME/ASCE/AHS 29th Structures, Structural Dynamics and Materials Conference, Williamsburg, VA, April 18-20, 1988. AIAA Paper No. 88-2337-CP. Also available as NASA TM-100569, March 1988.

8. Davis, M. W.: Optimization of Helicopter Rotor Blade Design for Minimum Vibration. NASA CP-2327, Part 2, September 1984, pp. 609-625.
9. Walsh, J. L.; Bingham, G. J.; and Riley, M. F.: Optimization Methods Applied to the Aerodynamic Design of Helicopter Rotor Blades. Journal of American Helicopter Society, October 1987, pp. 39-44.
10. Nixon, M. W.: Preliminary Structural Design of Composite Main Rotor Blades for Minimum Weight. NASA TP-2730, July 1987.
11. Rao, S. S.: Multiobjective Optimization in Structural Design with Uncertain Parameters and Stochastic Processes. AIAA Journal, Vol. 22, No. 11, November 1984.
12. Vanderplaats, G. N.: CONMIN - A Fortran Program for Constrained Function Minimization. User's Manual. NASA TMX-62282. August 1973.
13. Sobieszczanski-Sobieski, J.: On the Sensitivity of Complex, Internally Coupled Systems. NASA TM-100537, January 1988.
14. Johnson, Wayne: A Comprehensive Analytical Model of Rotorcraft Aerodynamics and Dynamics. NASA TM 81182, 1980.
15. Walsh, Joanne L.: Applications of Numerical Optimization Procedures to a Structural Model of a Large Finite-Element Wing. NASA TM 87597, 1986.

16. Bingham, Gene J.: The Aerodynamic Influences of Rotor Blade Airfoil, Twist, Taper, and Solidity on Hover and Forward Flight Performance. 37th Annual Forum of the American Helicopter Society. New Orleans, Louisiana, May 1981.
17. Gessow, Alfred; and Myers, Garry C., Jr.: Aerodynamics of the Helicopters. Frederick Unger Publishing Company, New York, 1952.
18. Strawn, Roger C.; and Tung, Chee: Prediction of Unsteady Transonic Rotor Loads With A Full-Potential Rotor Code. 43rd Annual Forum of the American Helicopter Society. St. Louis, Missouri, May 1987.
19. Berry, John D.: Quarter Scale Testing of an Advanced Rotor System for the UH-1 Helicopter. 37th Annual Forum of the American Helicopter Society. New Orleans, Louisiana, May 1981.
20. Kelley, Henry L.; and Wilson, John C.: Aerodynamic Performance of a 27-Percent-Scale AH-64 Wind-Tunnel Model With Baseline/ Advanced Rotor Blades. 41st Annual Forum of the American Helicopter Society. Ft. Worth, Texas, May 1985.
21. Kelley, Henry L.: Effect of Planform Taper on Hover Performance of an Advanced AH-64 Model rotor. NASA TM 89145, 1987.
22. Yeager, W. T.; Mantay, W. R.; Wilbur, M. L.; Cramer, R. G., Jr.; and Singleton, J. D.: Wind-Tunnel Evaluation of an Advanced Main-Rotor Blade Design for a Utility-Class Helicopter. NASA TM 89129, 1987.

23. Pritchard, J. I.; and Adelman, M. M.: Optimal Placement of Tuning Masses for Vibration Reduction in Helicopter Rotor Blades. Presented at the Second International Conference on Rotocraft Basic Research, College Park, Md., February 1988.
24. Whetstone, W. D.: EISI-EAL Engineering Analysis Language Reference Manual. Engineering Information Systems, Inc., San Jose, CA, 1983.
25. Jones, Robert M.: Mechanics of Composite Materials. Scripta Book Co., Washington, DC, 1975.
26. MIL-S-8698, Structural Design Requirements, Helicopters, August 1950.
27. Department of the Army: Engineering Design Handbook, Helicopter Engineering, Part One, Preliminary Design. AMC PAMPHLET No. 706-201, August 1974.
28. Brentner, K. S.: Prediction of Helicopter Rotor Discrete Frequency Noise - A Computer Program Incorporating Realistic Blade Motions and Advanced Acoustic Formulation. NASA TM-87721, October 1986.
29. Ffowcs Williams, J. E.; and Hawkings, D. L.: Sound Generation by Turbulence and Surfaces in Arbitrary Motion. Philos. Trans. R. Soc. London, ser. A, vol. 264, no. 1151, May 8, 1969, pp. 321-342.
30. Lighthill, M. J.: On Sound Generated Aerodynamically. I. General Theory. Proc. R. Soc. (London), ser. A, vol. 211, no. 1107, Mar. 20, 1952, pp. 564-587.
31. Farassat, F.; and Succi, G. P.: The Prediction of Helicopter Rotor Discrete Frequency Noise. Vertica, vol. 7, no. 4, 1983, pp. 309-320.

32. Farassat, F.: Theory of Noise Generation From Moving Bodies With an Application to Helicopter Rotors. NASA TR R-451, 1975.
33. Farassat, F.: Advanced Theoretical Treatment of Propeller Noise. Propeller Performance and Noise, VKI-LS 1982-08, Volume 1, Von Karman Inst. Fluid Dyn., May 1982.
34. Coleman, R. P.; and Feingold, A. M.: Theory of Self-Excited Mechanical Oscillations of Helicopters With Hinged Blades. NACA Report 1351, 1958.
35. Donham, R. E.; Cardinale, S. V.; and Sachs, I. B.: Ground and Air Resonance Characteristics of a Soft-Inplane Rigid-Rotor System. Journal of the American Helicopter Society, vol. 14, no. 4, October 1969, pp. 33-41.
36. Wood, E. R.; and Buffalano, A. C.: Parametric Investigation of the Aerodynamic and Aeroelastic Characteristics of Articulated and Rigid (Hingeless) Helicopter Rotor Systems. U.S. Army TRECOM Technical Report 64-15, April 1964.
37. Gerstenberger, W.; and Wood, E. R.: Analysis of Helicopter Aeroelastic Characteristics in High-Speed Flight. AIAA J., vol. 1, no. 10, Oct. 1963, pp. 2366-2381.
38. Novak, M. E.: Rotating Elements in the Direct Stiffness Method of Dynamic Analysis With Extensions to Computer Graphics. Shock and Vibration Bulletin, Bull. 40, Pt. 4, Oct. 1969, pp. 41-46.
39. Staley, J. A.; and Sciarra, J. J.: Coupled Rotor/Airframe Vibration Prediction Methods. Rotorcraft Dynamics, NASA SP-352, 1974, pp. 81-90.

40. Berry, J. D.; et al.: Helicopter Rotor Induced Velocities Theory and Experiment. American Helicopter Society Specialists Meeting on Aerodynamics and Aeroacoustics, February 1987.
41. Caradonna, F. X.; Lautenschlager, J. L.; and Silva, M. J.: An Experimental Study of Rotor-Vortex Interactions. Preprint from AIAA 26th Aerospace Sciences Meeting, January 1988.
42. Lake, R. C.; and Nixon, M. W.: Results From a Preliminary Investigation of Finite-Element Modeling in Analysis of Composite Rotor Blades. Second International Conference on Rotorcraft Basic Research, February 1988.
43. Althoff, S. L.: Effect of Advanced Rotorcraft Airfoil Sections on the Hover Performance of a Small Scale Rotor Model. NASA TP-2832 (AVSCOM TP-88-B-001) Sept. 1988.
44. Gardner, J. E.; and Dixon, S. C.: Loads and Aeroelasticity Division Research and Technology Accomplishments for FY 1984 and Plans for FY 1985. NASA TM 86356, 1985, pp. 138-139.
45. Mantay, W. R.; and Rorke, J. B.: The Evolution of the Variable Geometry Rotor. American Helicopter Society Symposium on Rotor Technology Proceedings, August 1976.
46. Bingham, Gene J.: The Aerodynamic Influences of Rotor Blade Taper, Twist, Airfoils and Solidity on Hover and Forward Flight Performance. 37th Annual Forum of the American Helicopter Society. New Orleans, Louisiana, May 1981.

47. Van Gaasbeck, J. R.: Rotorcraft Flight Simulation, Computer Program C81.  
USARTL-TR-77-54B, 1979.

TABLE 1.- SUMMARY OF DESIGN VARIABLES

Description	Symbol
Tuning mass at location i	$m_i$
Spanwise location of i-th mass	$x_i$
Wing box dimensions	$t_1, t_2, t_3$
Ply thicknesses	$t_{45}, t_0$
Depth of blade at root	$h_r$
Ratio of blade depths at tip and root	$\lambda_h = h_r/h_t$
Maximum pre-twist of blade	$\tau_{max}$
Percent blade span where taper begins	$r$
Blade root chord	$c_r$
Airfoil distribution	-
Hinge offset	$e$
Blade angular velocity	$\Omega$
Number of blades on rotor	$N$
Blade radius	$R$
Ratio of root chord to tip chord	$\lambda_c = c_r/c_t$

TABLE 2.- SUMMARY OF CONSTRAINTS

Constraint Description	Form of Constraint	Comments
Main rotor horsepower	$HP_i \leq \text{HP avail for } i\text{-th condition}$	For 5 flight conditions Enforced at 12 azimuthal locations
Airfoil section stall	$C_D \leq C_{Dmax}$	
Blade frequencies Blade vertical load Blade inplane load Transmitted in-plane hub shears Hub pitching moment Hub rolling moment Blade response amp. Autorotational inertia Aeroelastic stability	$f_{il} \leq f_i \leq f_{iu}$ $V_{ik} \leq V_{max}$ $H_{ik} \leq H_{max}$ $X_k \leq X_{max}$ $Y_k \leq Y_{max}$ $P_k \leq P_{max}$ $R_k \leq R_{max}$ $Q_k \leq Q_{max}$ $\Sigma m - 2 \geq \alpha$ $Re \leq -\epsilon$	
Wing box stresses	$R \leq 1$	R - TSai-Hill criterion
Blade tip deflection Blade twist	$w \leq w_{max}$ $\theta \leq \theta_{max}$	
Blade tip Mach no. Blade thickness	$M \leq M_{max}$ $h \leq h_{max}$	Limits thickness noise
Blade lift distribution	$dC_l/dx \leq S_{max}$	Limits BVI & loading noise
Ground resonance Rotor/Airframe frequency coupling	$ \Omega - \omega_{L1}  < \omega_{af}$ $f_1 \leq N\Omega \leq f_u$	Effective airframe constraint

TABLE 3.- INTERACTIONS AMONG DISCIPLINES

Variable	Acoustics	Aerodyn. (Perf & Loads)	Dynamics	Structures	Fuselage Dynamics
Airfoil Dist.	S	S	W	W	W
Planform	S	S	S	S	S/W
Twist	W	S	S	W	W
Tip speed	S	S	S	S	S
Blade number	S	W	S	W	S
Stiffness	W	S	S	S	S/W
Mass dist.	W	W	S	S	S/W
Hinge offset	W	W	S/W	W	S/W

S - Strong interaction

W - Weak interaction

TABLE 4.- CANDIDATE TASK AND MISSION FOR PHASE 1 DESIGN ACTIVITY

4000 ft 95° Condition	
Aircraft gross weight	16875 lb
Installed power limit	3400 HP
$V_{\text{cruise}}$	140 kts
$V_{\text{max}}$	200 kts
g's at 120 kts	3.5
Vertical rate of climb	1000 fpm
Airframe structure	UH-60B

Other constraints and guidelines are specified in table 2.

TABLE 5.- OPTIMIZATION RESULT FOR RECTANGULAR AND TAPERED BLADES

	Reference blade	Optimum blade	
		Rectangular 30 d.v.	Tapered 42 d.v.
$\lambda_h$	1.0	1.0	1.49
$f_1$ , Hz	12.285	12.408*	12.408*
$f_2$ , Hz	16.098	16.056	16.066
$f_3$ , Hz	20.913	20.968	20.888
$f_4$ , Hz	34.624	34.546	34.678
$f_5$ , Hz	35.861	35.502*	35.507
Authorotational inertia, lb-ft <sup>2</sup>	517.3	517.3*	517.3*
Blade weight, lbm	98.27	95.62	92.16
Percent reduction in blade weight**	---	2.67	6.21

\*\*-From reference blade

\*-Active constraint

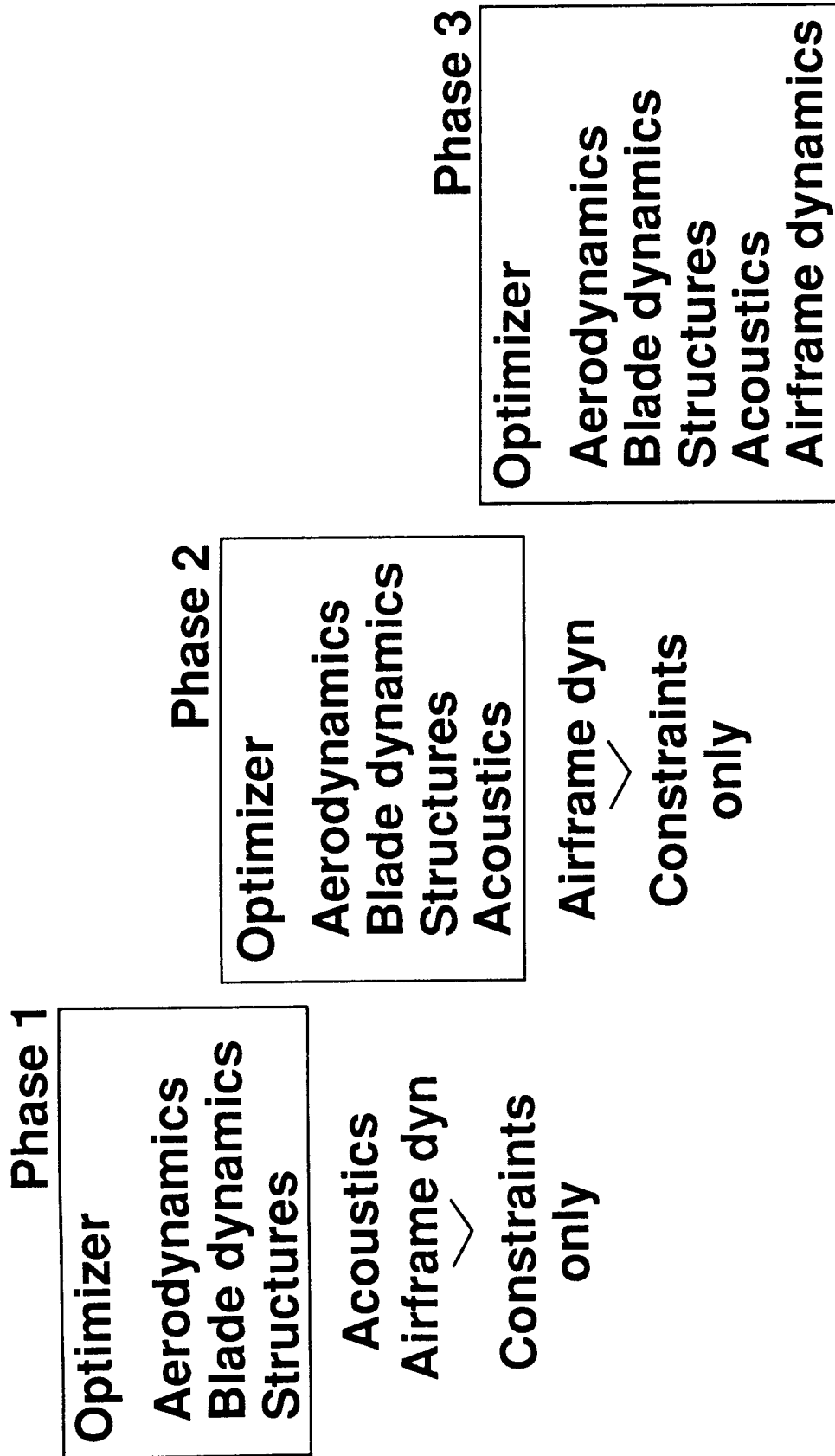


Figure 1.- Phased Approach to Development of Integrated Rotorcraft Optimization Procedures.

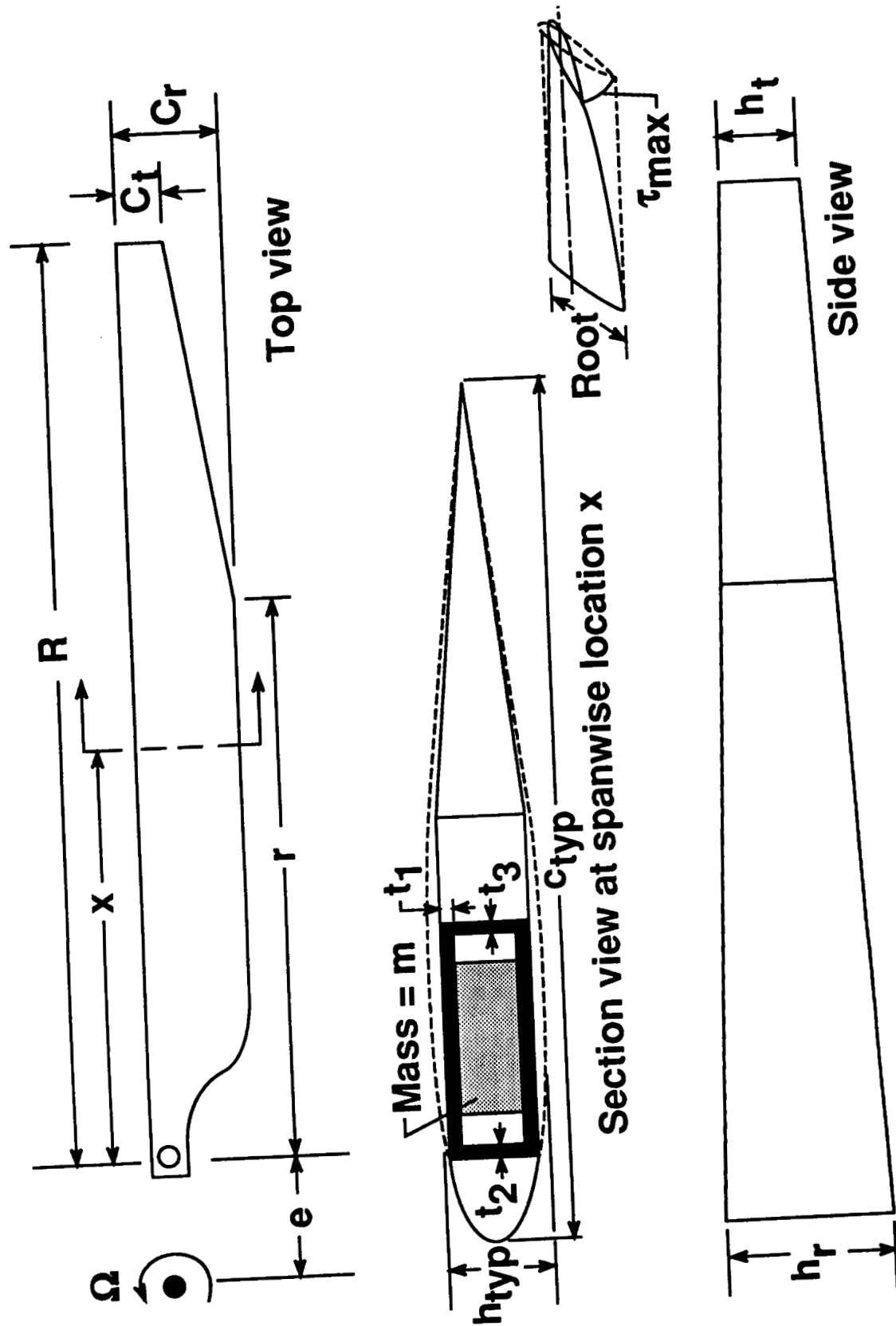


Figure 2.- Blade Model and Design Variables.

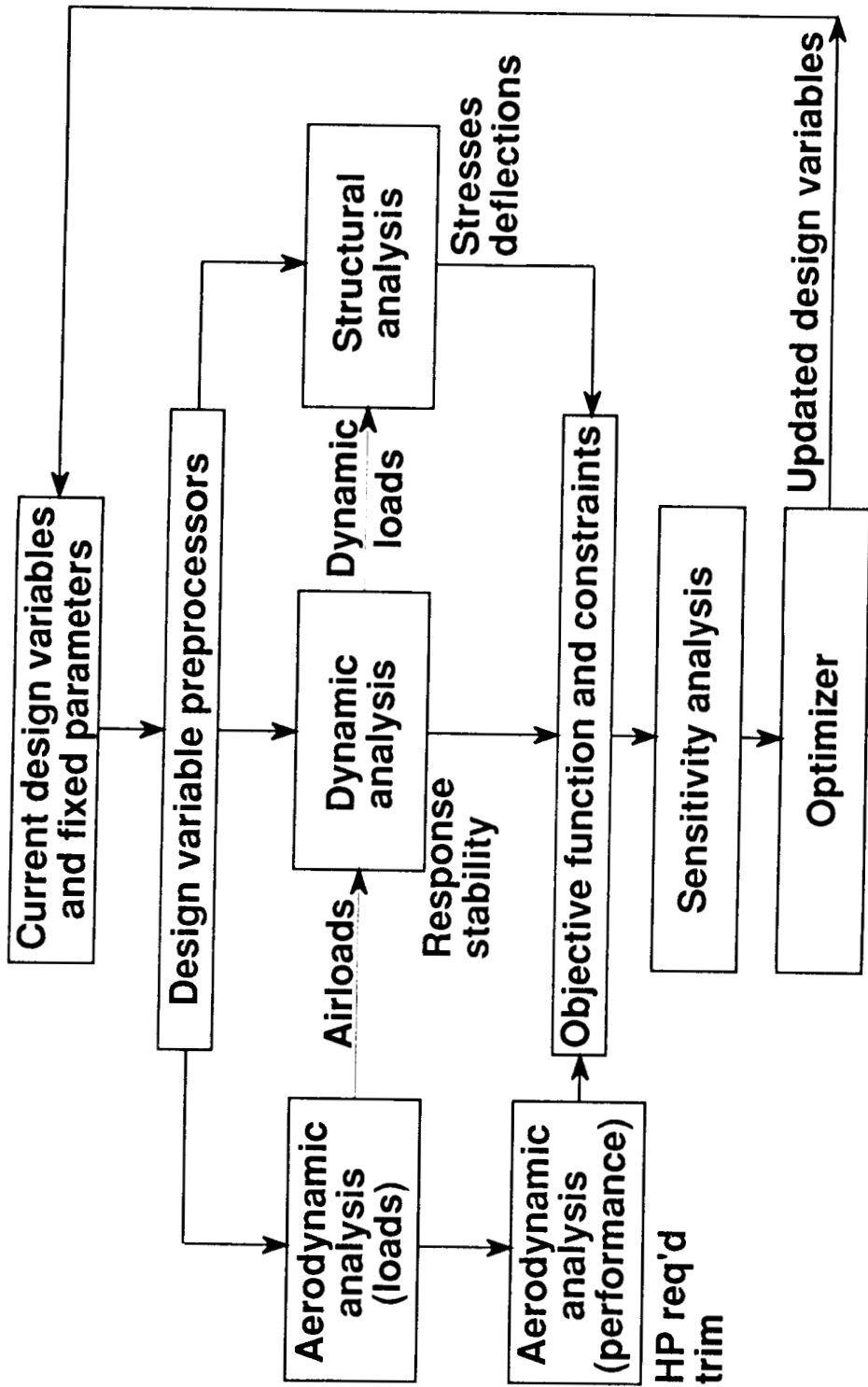


Figure 3.- Integrated Aerodynamic-Dynamic-Structural Optimization of Rotor Blades.

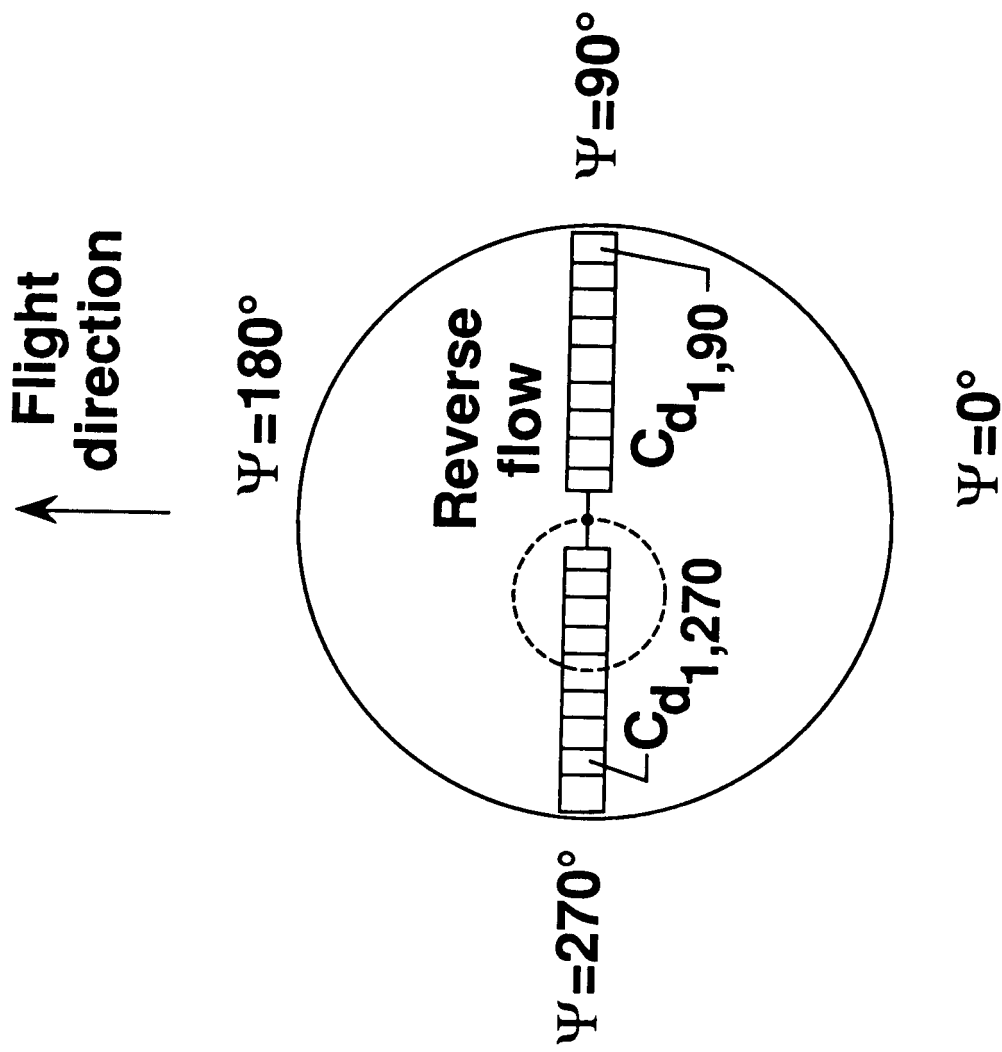


Figure 4.- Schematic Diagram Used to Establish Airfoil Section Stall Constraint.

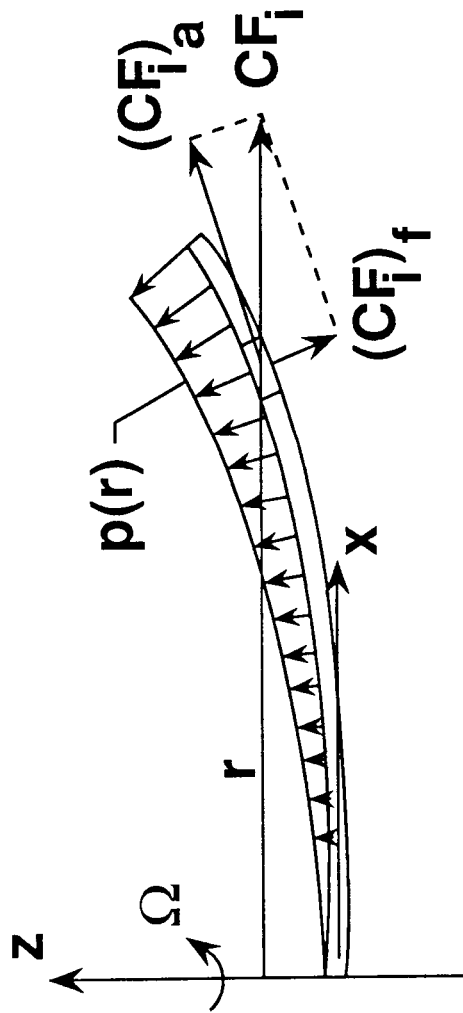


Figure 5.- Interaction of Flapwise and Centrifugal Loads Acting on Rotor Blade Model.

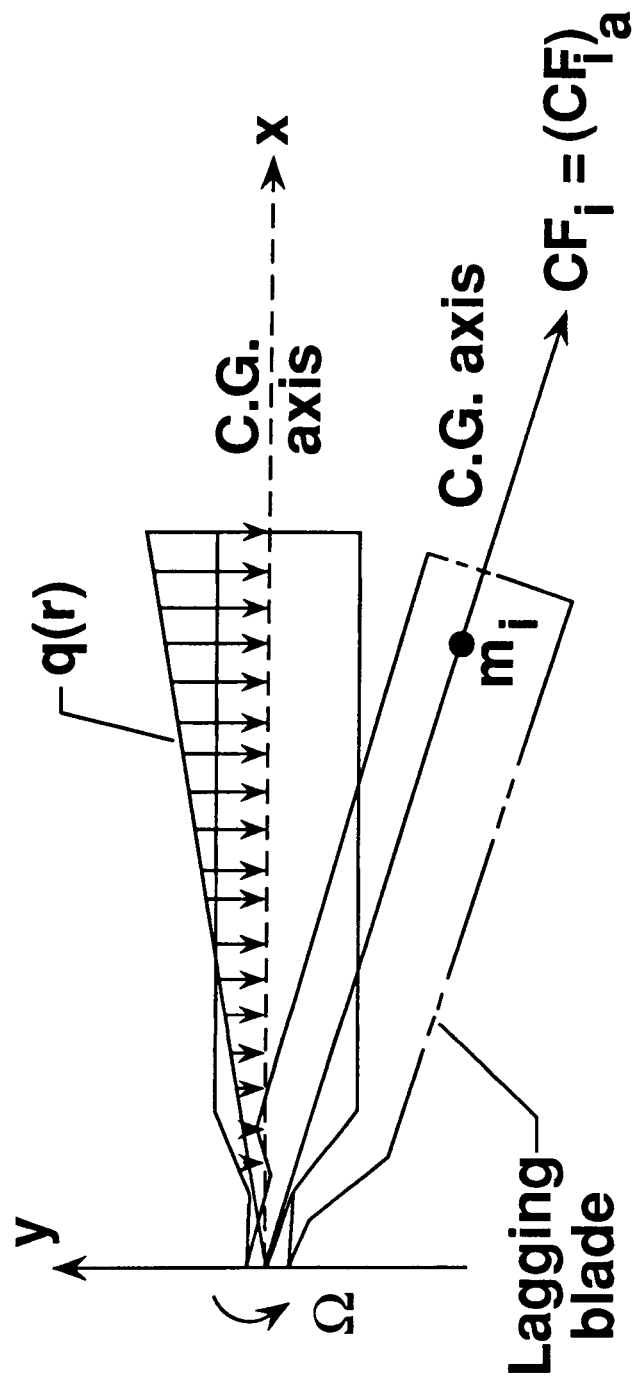


Figure 6.- Interaction of In-Plane and Centrifugal Loads Acting on a Rotor Blade Model.

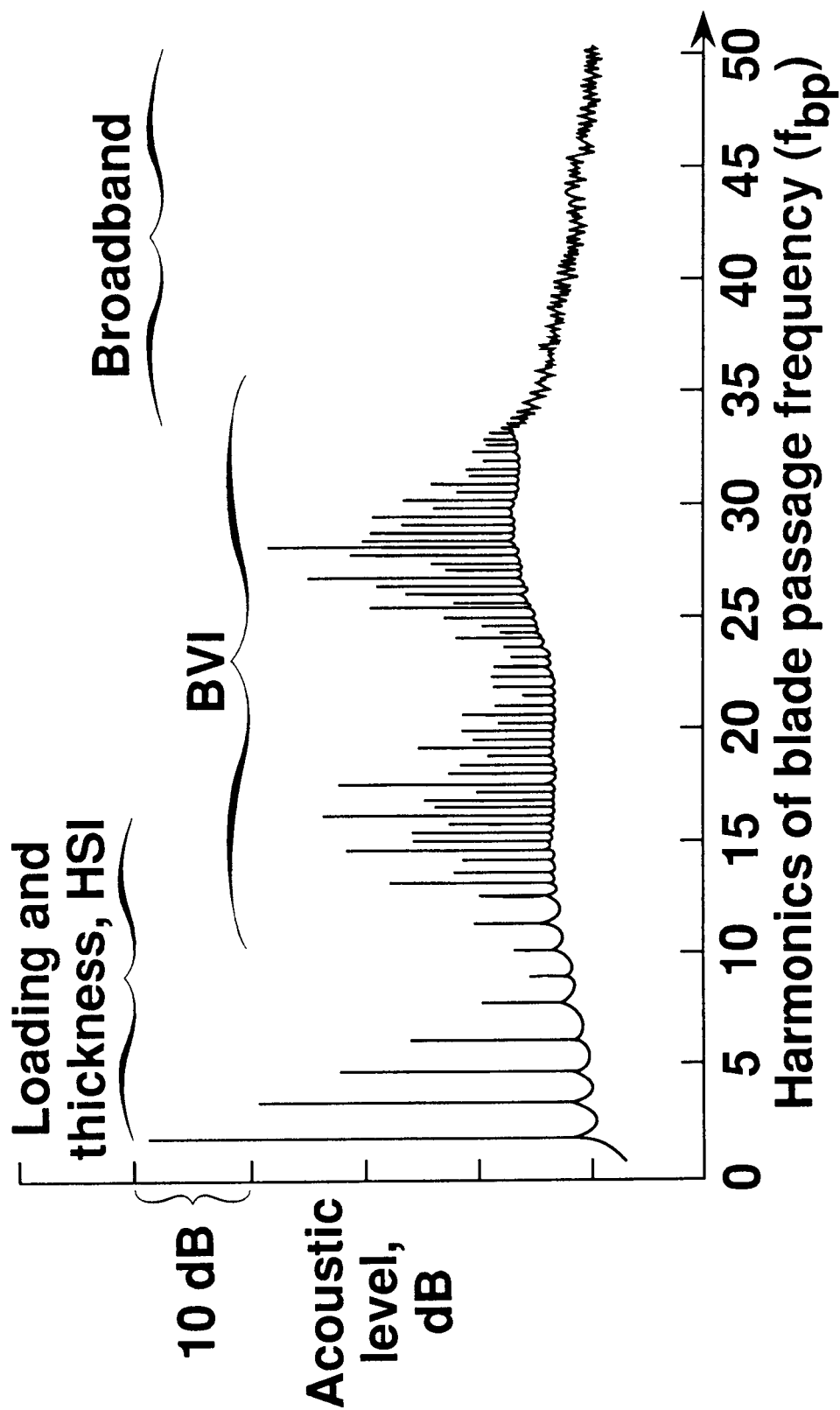


Figure 7.- Illustration of Frequency Ranges of the Major Rotor Noise Sources.

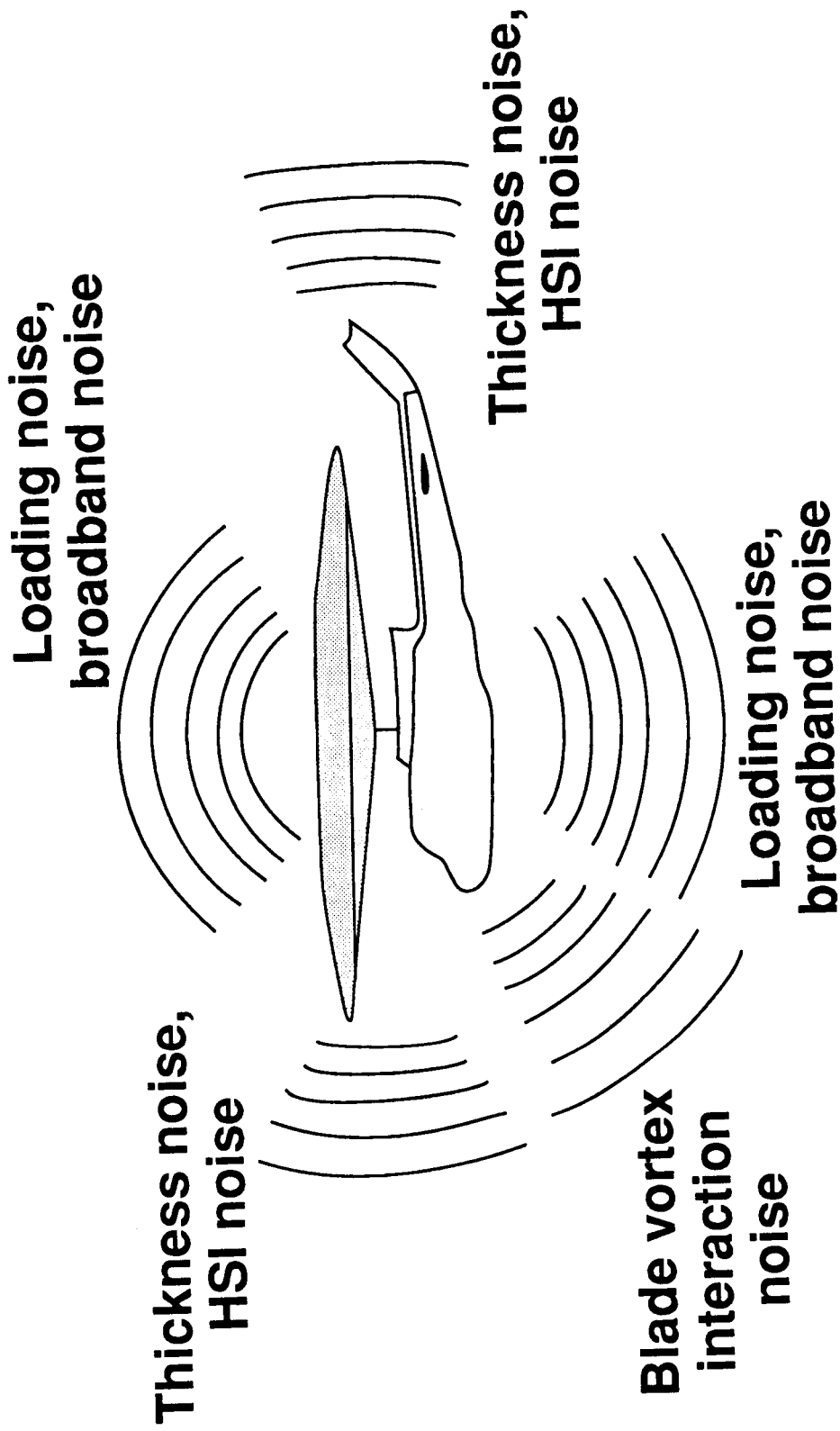


Figure 8. - Illustration of the General Directivity Patterns of the Major Rotor Noise Sources.

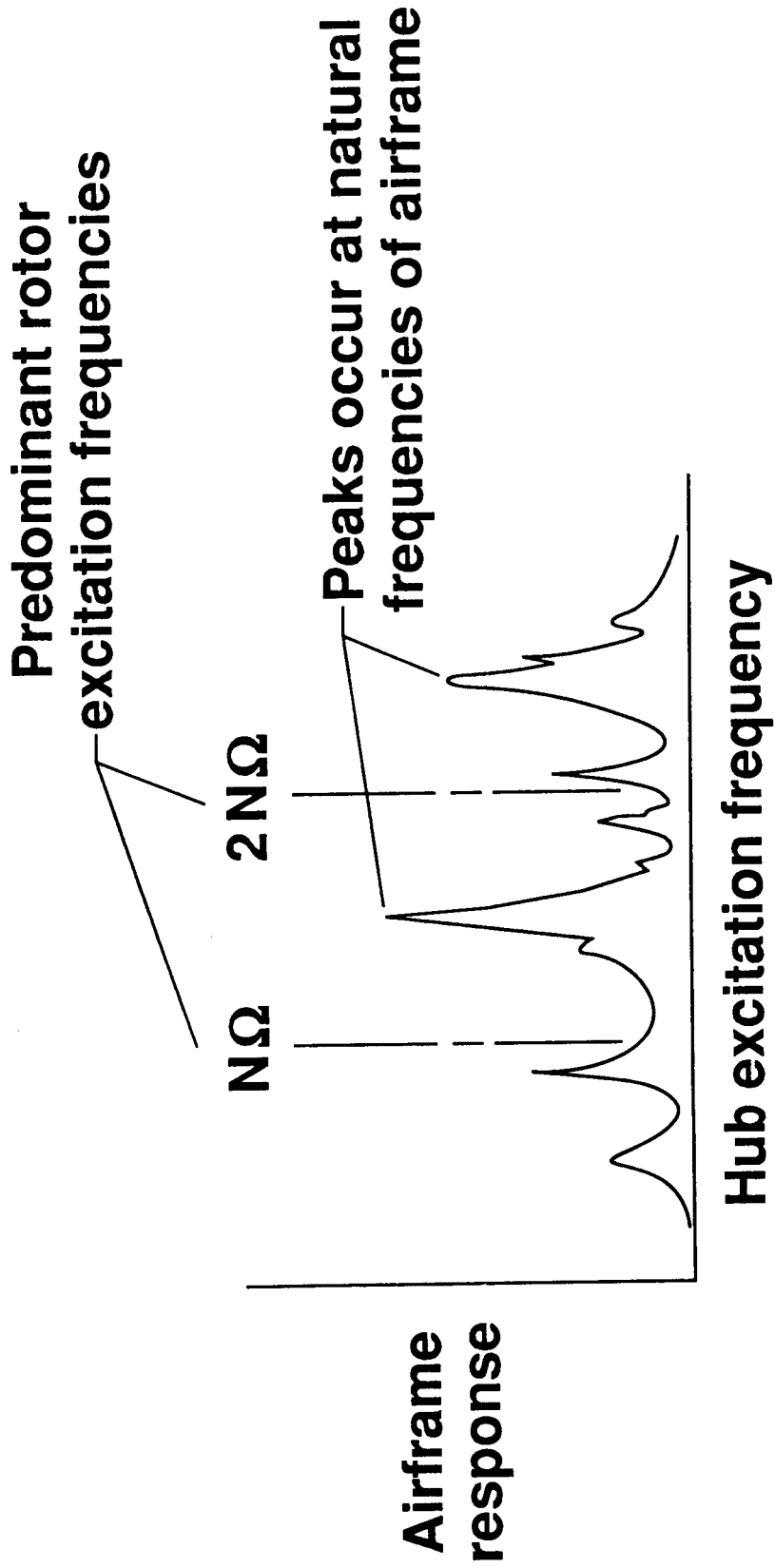
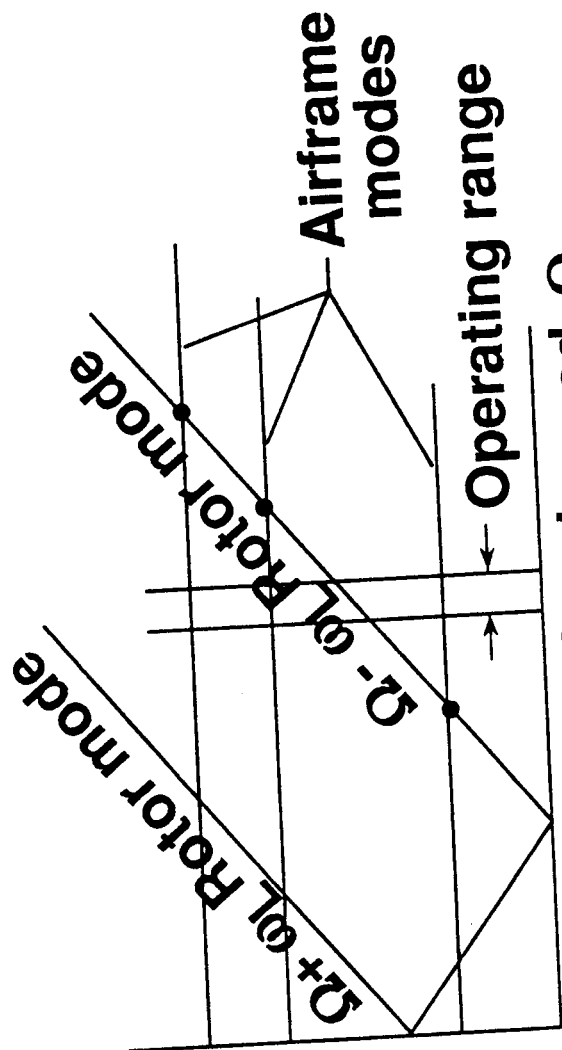
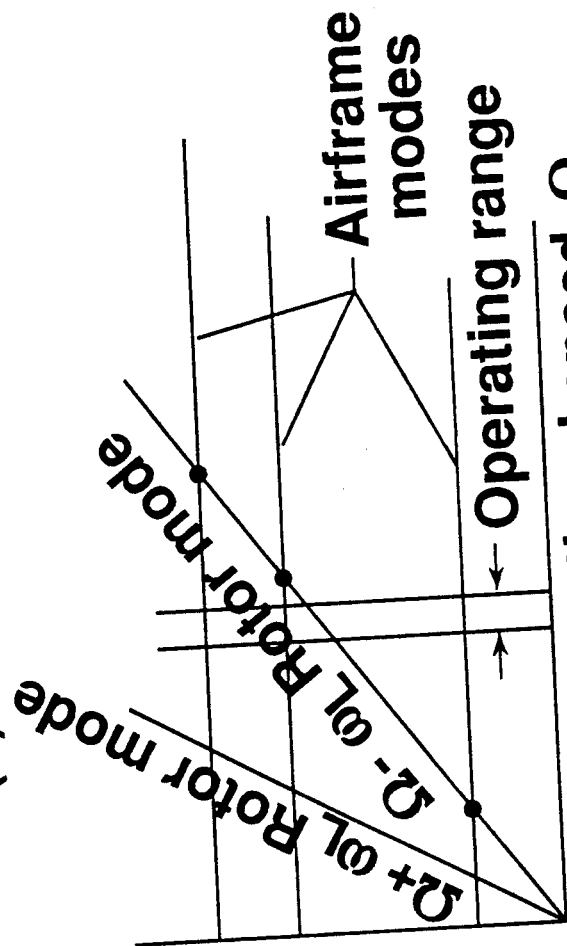


Figure 9. - Typical Variation of Airframe Response With Hub Excitation Frequency.



(a) Hingeless rotor



(b) Articulated rotor

Figure 10.- Typical Variation of Uncoupled Rotor and Airframe Frequencies With Rotor Rotational Speed for Assessment of Ground and Air Resonance.

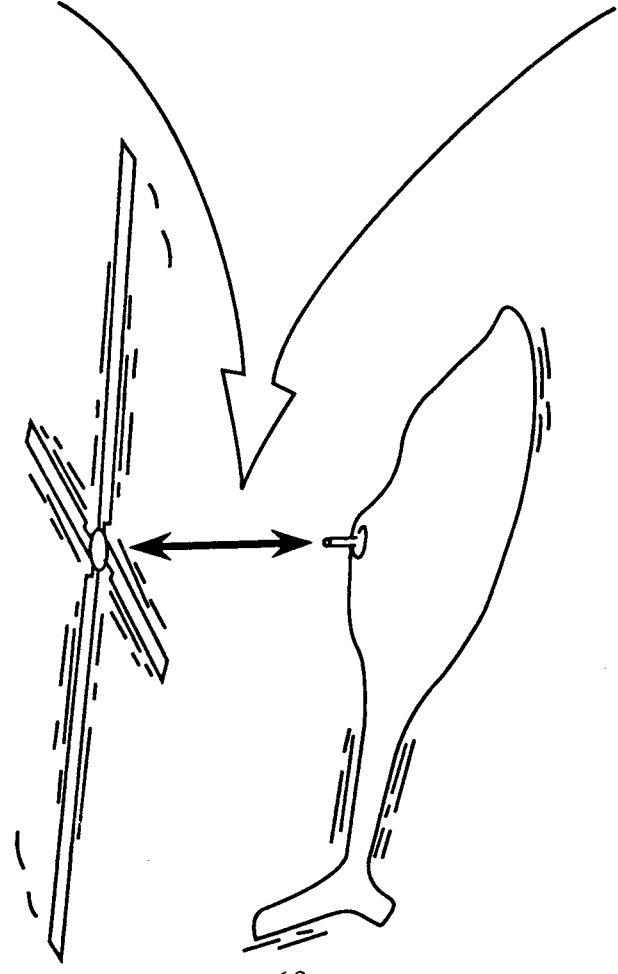
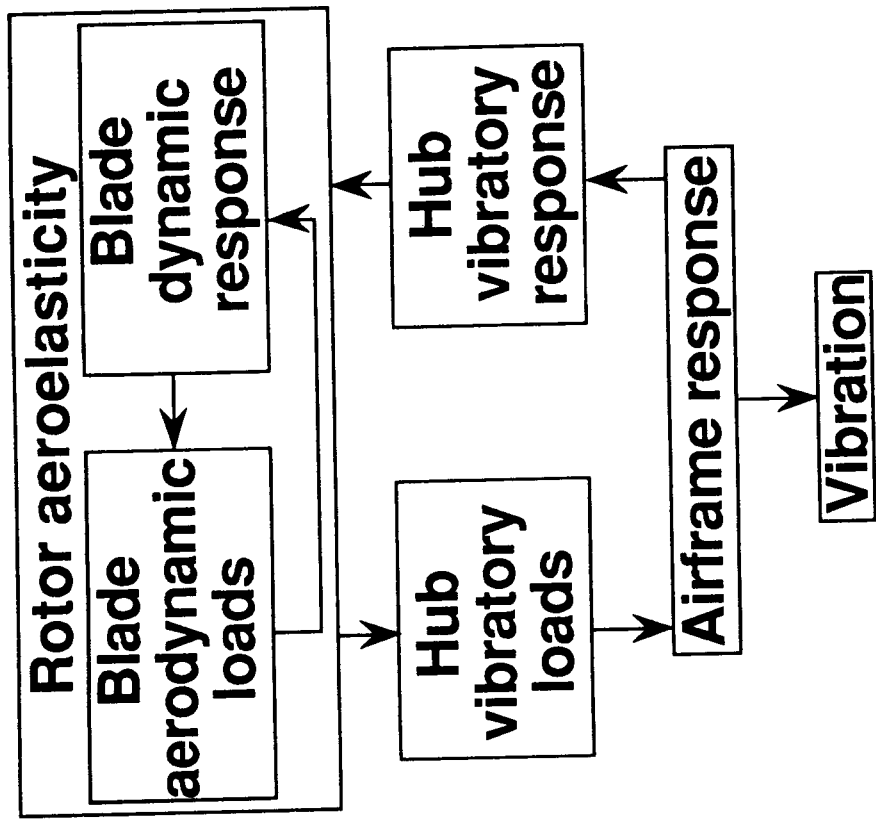


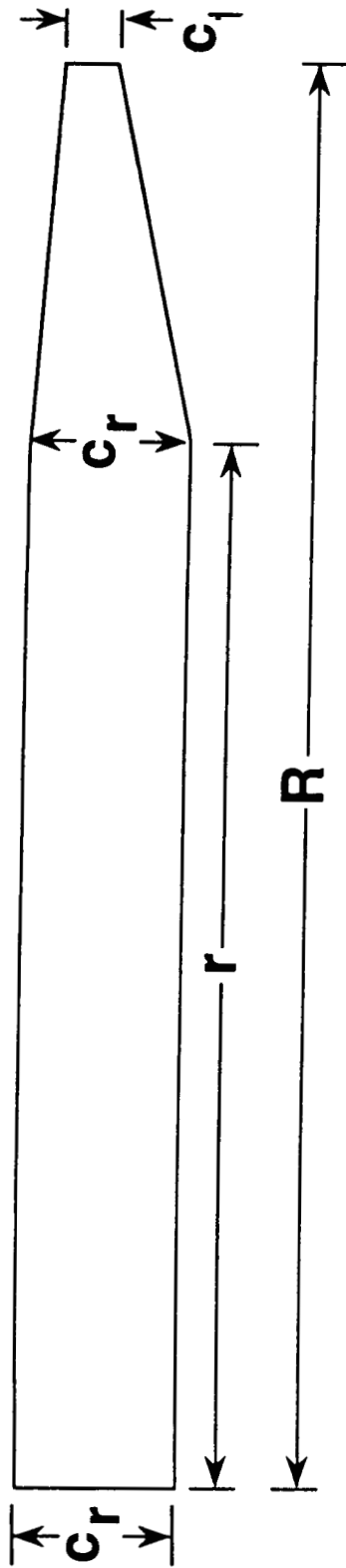
Figure 11.- A Simplified View of Rotor-Airframe Interaction in Producing Vibrations.

	FY 88	89	90	91	92	93	
Phase 1	1	3	6	Disciplinary optimization			
	2	5	8	10	13	18	
	Validation			4	11	14	17
				12	19	23	
Phase 2	Incorporate acoustics			7	9	15	
Phase 3	Incorporate airframe dynamics			16	20	22	

**Milestones:**

- |                          |                               |                            |
|--------------------------|-------------------------------|----------------------------|
| 1 Dynamic optimization   | 9 Incorporate WOPWOP code     | 17 Airframe dyn sens       |
| 2 Aero Load/Dyn opt      | 10 Acoustics constraints      | 18 Complete phase 1 dev    |
| 3 Performance opt        | 11 Aerodynamic sens analysis  | 19 Design test article     |
| 4 Apply Dyn opt to GBH-T | 12 Specs for test article     | 20 Rotor/AF coupling       |
| 5 Full Aero/Dyn opt      | 13 Airframe constraints       | 21 Complete phase 2        |
| 6 Structural opt         | 14 Acoustic sens analysis     | 22 Incorp AF sens analysis |
| 7 Formulate Phase 2      | 15 Incorp acous sens analysis | 23 Fabricate test article  |
| 8 Aero/Dyn/Struc opt     | 16 Formulate phase 3          | 24 Test article in TDT     |

Figure 12.- Development Schedule and Milestones for Integrated Rotorcraft Optimization.



Point of taper initiation  $r$   
 Root chord  $c_r$   
 Taper ratio  $c_r/c_t$

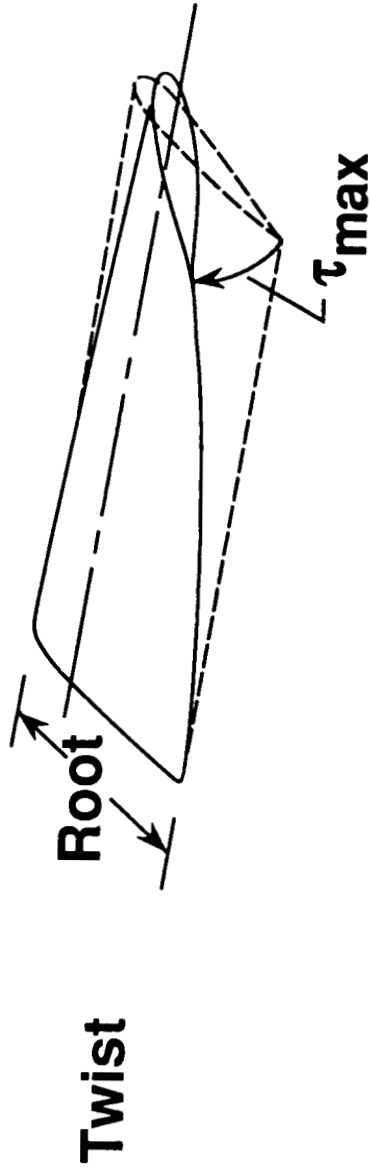
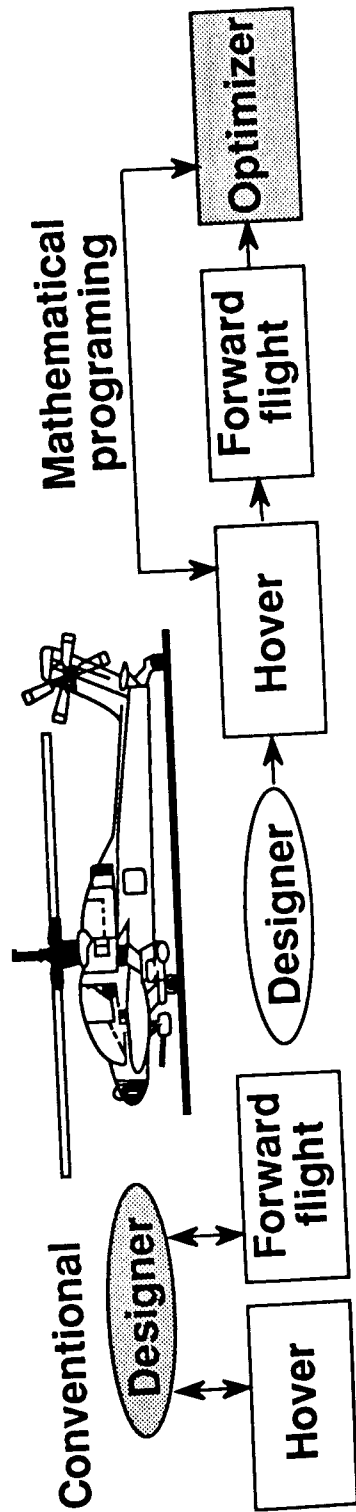


Figure 13.- Rotor Blade Design Variables for Aerodynamic Performance.



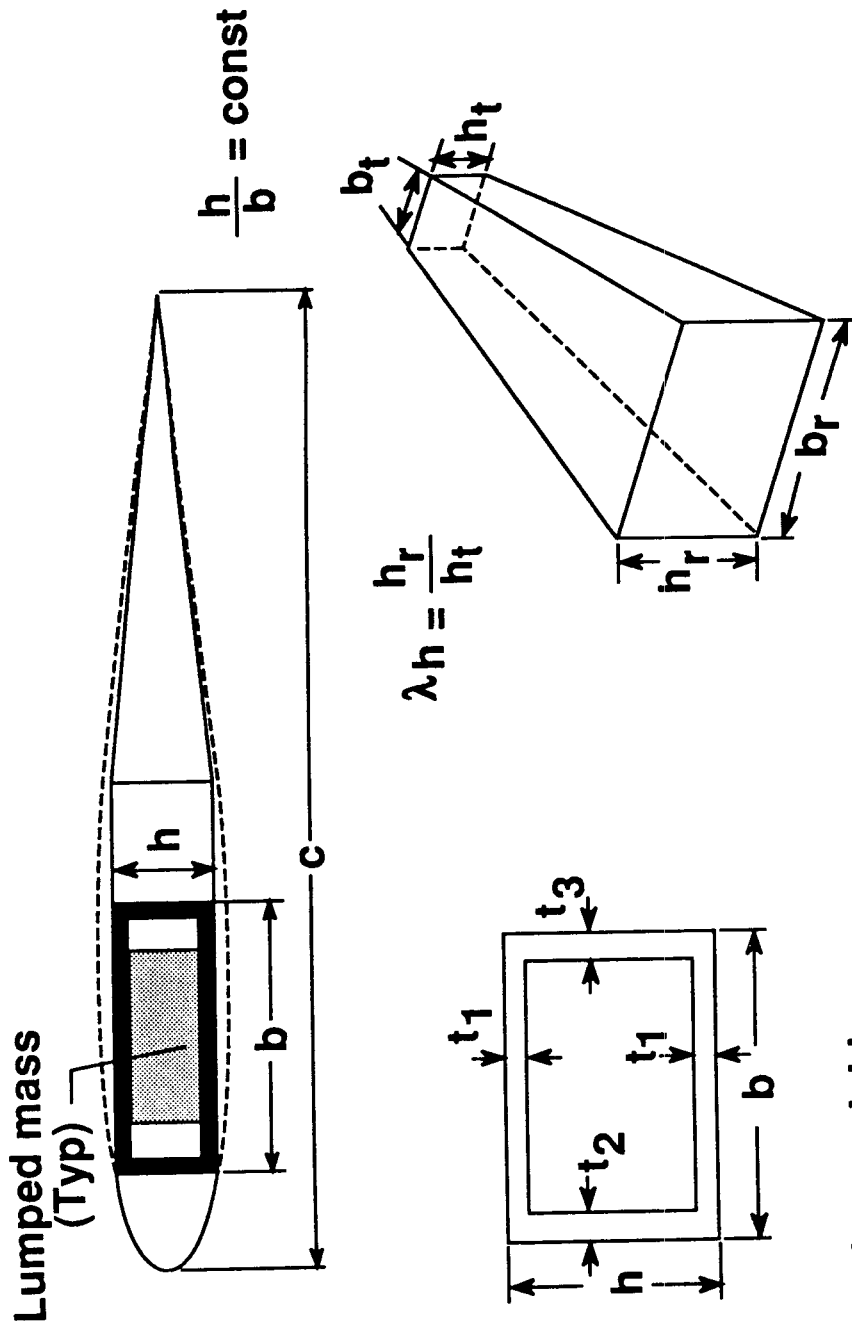
Objective function: Hover horsepower

Design variables { Twist, deg  
Percent taper  
Taper ratio  
Root chord, ft

Design time

1558 hp	1533 hp
-12	-15
.80	.91
3.0	3.1
2.3	1.78
5 weeks	2 days

Figure 14.- Results of Aerodynamic Performance Optimization.



- Design variables
  - Box beam wall thicknesses,  $t_1, t_2, t_3$  (at spanwise positions)
  - Box beam outer dimension  $h_r$
  - Taper ratio  $\lambda h$
  - Magnitudes of lumped masses (at spanwise positions)

Figure 15.- Model and Design Variables for Dynamic Optimization Example.

- Minimize: Blade weight  $W$

$$W = W_b + W_o$$

$$= \sum_{j=1}^N \rho_j A_j L_j + \sum_{j=1}^N W_{o_j}$$

$W_b$  = box beam weight

$W_o$  = nonstructural

- Constraints

$$\text{Frequency } f_{k_L} \leq f_k \leq f_{k_U}$$

$$k = 1, 2, \dots, 5$$

(elastic modes only)

$$\text{Autorotational inertia } \sum_{j=1}^N W_j r_j^2 \geq \alpha$$

$\alpha$ : minimum prescribed rotary inertia

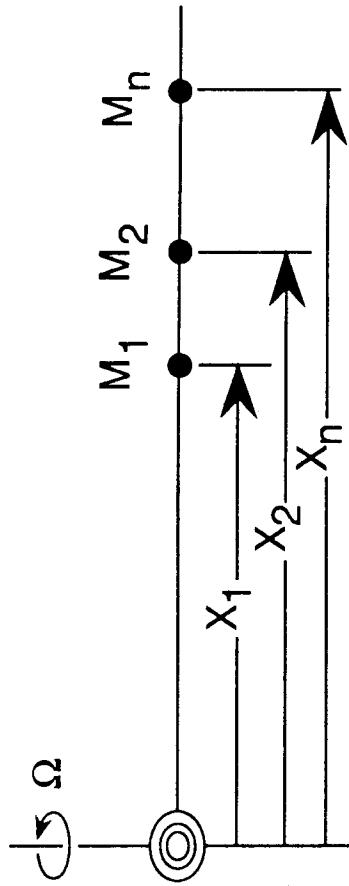
$$\text{Stress } \left( \sum_{j=k}^N M_j \Omega^2 r_j / A_k \right) \cdot FS \leq \sigma_{\max}$$

$\underbrace{\hspace{10em}}_{\sigma_k}$

$$\text{Side } \phi_{i_L} \leq \phi_i \leq \phi_{i_U}$$

$\phi_i$ :  $i$ th design variable

Figure 16.- Mathematical Formulation of Optimization for Dynamics.



- **Design goal - Find optimum combination of masses and their locations to reduce blade root vertical shear**
- **Method - Formulate optimization procedure**
  - **Use masses and locations as design variables**
  - **Minimize -**
    - **Blade root vertical shear**
    - **Added mass**

Figure 17.- Selection of Optimum Locations of Tuning Masses for Vibration Reduction.

5.21 6.55 6.60 (lbm)  
 135 154 174 (in)

Initial masses  
 and locations

7.1 5.2 .97 (lbm)  
 135 146 157 (in)

Final masses  
 and locations

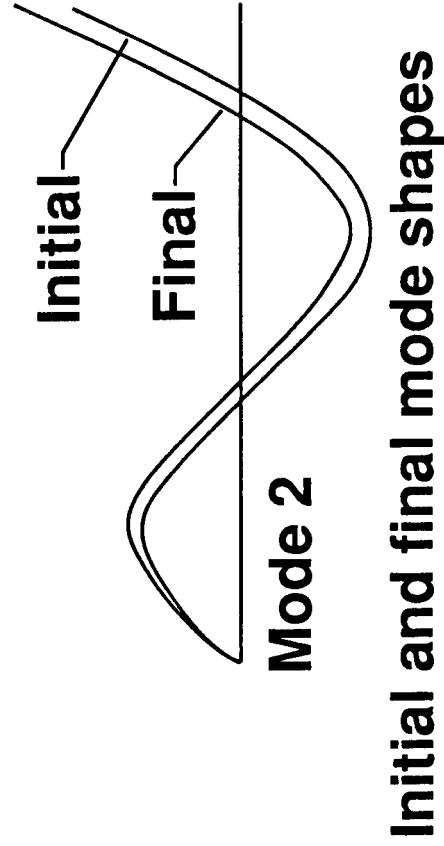
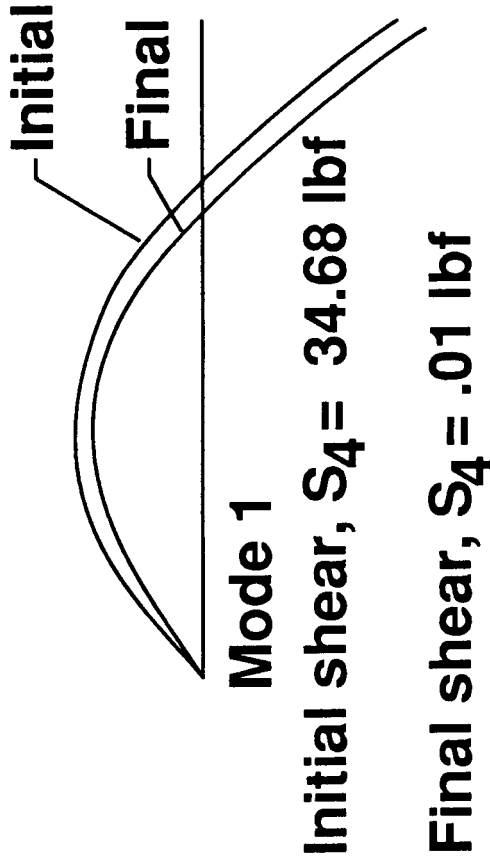


Figure 18.- Initial and Final Designs - Minimized 4/rev Vertical Shear for 2 Modes.

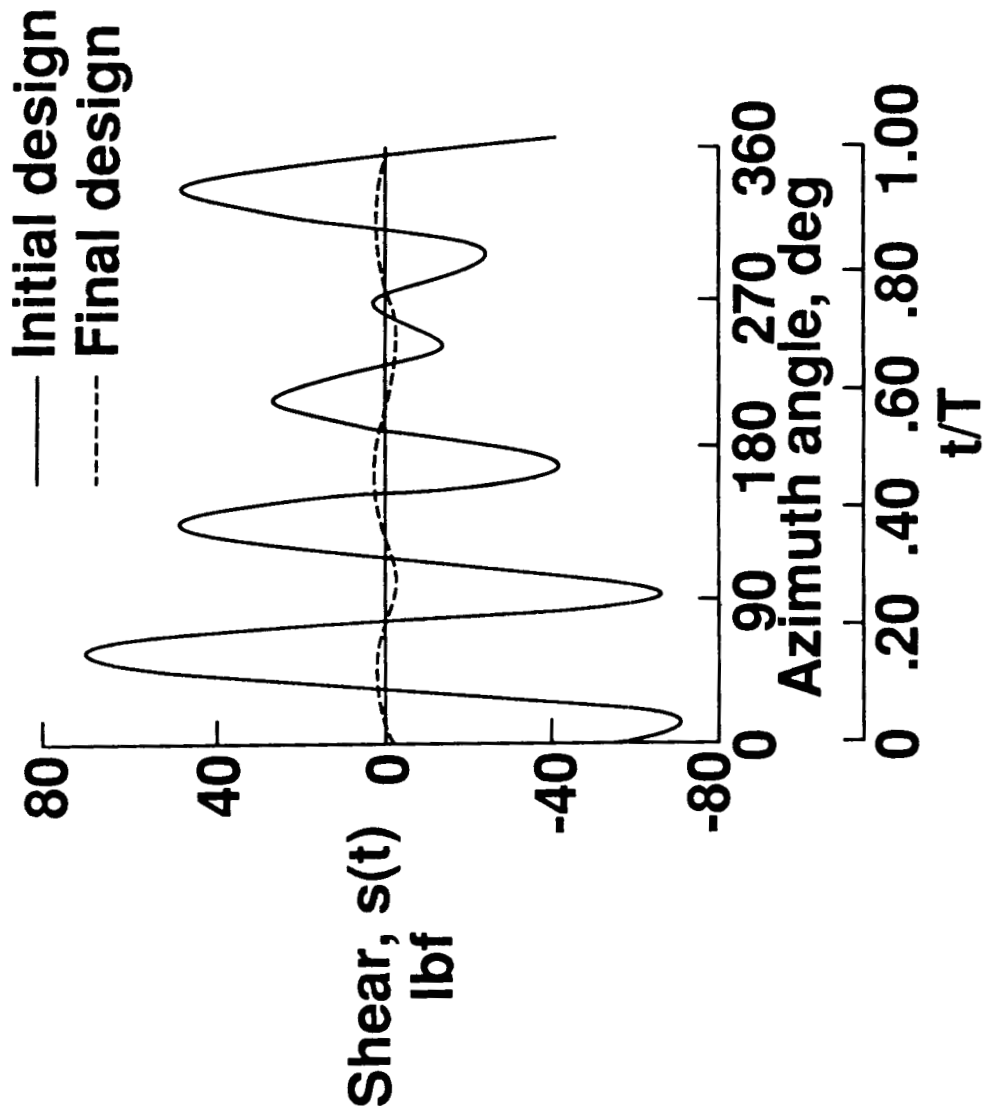
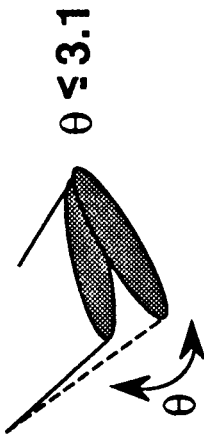


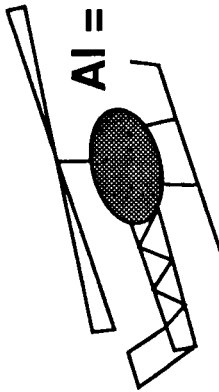
Figure 19.- Time History of Vertical Root Shear Minimized for 2 Modes/3 Harmonics.

**Twist constraint**



$$\theta \leq 3.1$$

**Autorotation constraints**



$$AI = \frac{I\Omega^2}{1100 \text{ hp}} > 1.7$$

**Material strength constraints**



$$1 - \bar{R} \geq 0$$

$\bar{R}$  = Tsai-Hill failure criterion

**Results**

Parameter	Actual		Metal Comp.	
	UH-60A	Ti spar	Ti spar	Gr/E spar
Spar mat.	Ti	---	Ti	Gr/E
Spar thick., in.	0.135	0.130	0.130	0.105
45° plys, %	---	---	---	20
Weight, lbs.	210	207	207	163
Margin (1-R)	---	0.103	0.103	0.000
Twist, deg.	---	0.92	0.92	2.55

**Design variables**

% of 45° plys (all others 0°)

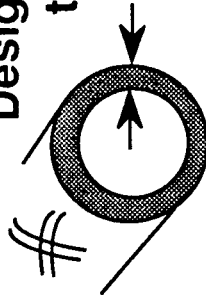


Figure 21.- Structural Optimization for Minimum Weight Rotor Blades.

- Objective function: Blade mass
- Constraints: Stress in skin and spars, twist deformation, autorotational inertia
- Design variables: Spar thicknesses, % of  $\pm 45^\circ$  plies

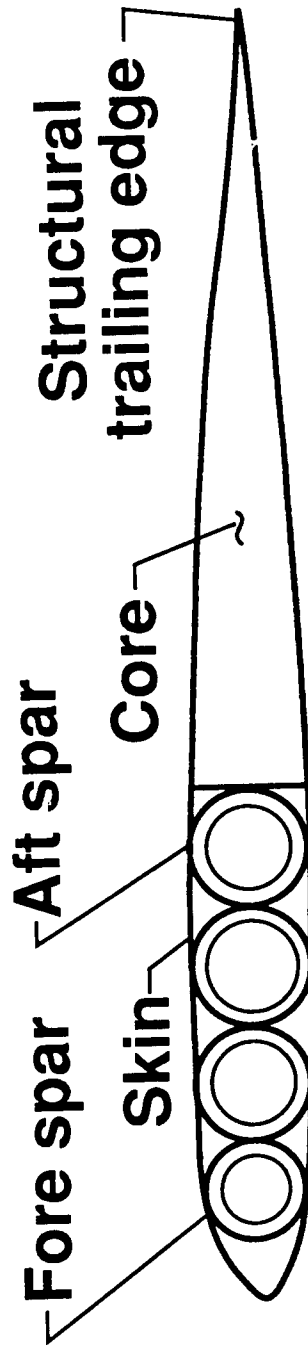


Figure 20.- Rotor Structural Optimization.



## Report Documentation Page

<b>1. Report No.</b> NASA TM-101617 AVSCOM TM-89-B-004	<b>2. Government Accession No.</b>	<b>3. Recipient's Catalog No.</b>
<b>4. Title and Subtitle</b> Integrated Multidisciplinary Optimization of Rotorcraft: A Plan for Development	<b>5. Report Date</b> May 1989	
	<b>6. Performing Organization Code</b>	
<b>7. Author(s)</b> Howard M. Adelman and Wayne R. Mantay, Editors	<b>8. Performing Organization Report No.</b>	
	<b>9. Performing Organization Name and Address</b> NASA Langley Research Center and Aerostructures Directorate USAARTA-AVSCOM Hampton, VA 23665-5225	
<b>12. Sponsoring Agency Name and Address</b> National Aeronautics and Space Administration Washington, DC 20546-0001 and U.S. Army Aviation Systems Command St. Louis, MO 63120-1798	<b>10. Work Unit No.</b> 505-63-51-10	
	<b>11. Contract or Grant No.</b>	
	<b>13. Type of Report and Period Covered</b> Technical Memorandum	
<b>14. Army Project No.</b>		
<b>15. Supplementary Notes</b> Authorship of sections in main body of the paper as follows: General Approach and Scope: Howard M. Adelman, NASA Langley Research Center; and Wayne R. Mantay, Aerostructures Directorate USAARTA-AVSCOM. Rotor Blade Aerodynamic Design: Joanne L. Walsh, NASA Langley Research Center; and Kevin W. Noonan, Aerostructures Directorate, USAARTA-AVSCOM. Rotor Blade Dynamic Design: Jocelyn I. Pritchard, Aerostructures Directorate, USAARTA-AVSCOM; Howard M. Adelman and Wayne R. Mantay. Rotor Blade Structural Design: Mark W. Nixon, Aerostructures Directorate, USAARTA-AVSCOM. Acoustic Design Considerations: Ruth M. Martin, NASA Langley Research Center. Airframe Design Considerations: Raymond G. Kvaternik, NASA Langley Research Center; and T. Sreekanta Murthy, Planning Research Corporation. Validation of Procedures: Wayne R. Mantay. Appendix-Results Obtained to Date: Joanne L. Walsh; Aditi Chattopadhyay, Analytical Services and Materials, Inc.; Jocelyn I. Pritchard; and Mark W. Nixon.		
<b>16. Abstract</b> This paper describes a joint NASA/Army initiative at the Langley Research Center to develop optimization procedures aimed at improving the rotor blade design process by integrating appropriate disciplines and accounting for important interactions among the disciplines. The paper describes the optimization formulation in terms of the objective function, design variables, and constraints. Additionally, some of the analysis aspects are discussed, validation strategies are described, and an initial attempt at defining the interdisciplinary couplings is summarized. At this writing, significant progress has been made, principally in the areas of single discipline optimization. Results in the paper describe accomplishments in rotor aerodynamic performance optimization for minimum hover horsepower, rotor dynamic optimization for vibration reduction, and rotor structural optimization for minimum weight.		
<b>17. Key Words (Suggested by Author(s))</b> Optimization      Aerodynamics Helicopters        Dynamics Rotor blades        Structural analysis	<b>18. Distribution Statement</b> Unclassified—Unlimited Subject Category 05	
<b>19. Security Classif. (of this report)</b> Unclassified	<b>20. Security Classif. (of this page)</b> Unclassified	<b>21. No. of Pages</b> 83
		<b>22. Price</b> A05